Quaternary Science Reviews 203 (2019) 102–127

Contents lists available at ScienceDirect

Quaternary Science Reviews

journal homepage: www.elsevier.com/locate/quascirev

Glacial lake evolution and Atlantic-Pacific drainage reversals during deglaciation of the Patagonian Ice Sheet

Varyl R. Thorndycraft [a, *], Jacob M. Bendle [a], Gerardo Benito [b], Bethan J. Davies [a], Carlos Sancho [c], Adrian P. Palmer [a], Derek Fabel [d], Alicia Medialdea [e], Julian R.V. Martin [a]

[a] Centre for Quaternary Research, Department of Geography, Royal Holloway University of London, Egham, TW20 0EX, UK
[b] Museo Nacional de Ciencias Naturales, Consejo Superior de Investigaciones Científicas, 28006, Madrid, Spain
[c] Department of Earth Sciences, University of Zaragoza, 50009, Zaragoza, Spain
[d] Scottish Universities Environmental Research Centre (SUERC), University of Glasgow, Scotland, UK
[e] Institute of Geography, University of Cologne, 50674, Cologne, Germany

ARTICLE INFO

Article history:
Received 12 June 2018
Received in revised form
30 August 2018
Accepted 30 October 2018
Available online 19 November 2018

Keywords:
Antarctic Cold Reversal
Bayesian age modelling
Cosmogenic isotopes
Glacial lake outburst floods (GLOFs)
Palaeohydrology
Palaeogeography
Palaeolake shorelines
Pleistocene
South America

ABSTRACT

Modelling experiments of drainage events from proglacial lakes of the Río Baker catchment (central Patagonia, 46–48 °S) indicate that Atlantic-Pacific drainage reversals may have caused freshwater forcing of regional climate. However, much of the region remains unmapped in detail and available geochronological data is equivocal, leading to multiple published palaeolake evolution models. We evaluate these models through new geomorphological mapping from the Baker valley; cosmogenic dating of moraine boulders that demonstrates an Antarctic Cold Reversal ice readvance that blocked drainage through the Río Baker; an altitudinal-based review of published geochronology; and regional analysis of shoreline glacio-isostasy and palaeolake levels. We use these datasets to present a new regional palaeolake evolution model underpinned by Bayesian age modelling. We demonstrate that 10^3 km^3 of freshwater was released to the Pacific over at least 6 drainage events from before 15.3–15.0 cal yr BP to the early Holocene. The final stages of lake drainage involved catastrophic flooding along the Baker valley, evidenced by high magnitude flood landforms such as boulder bars, likely caused by failure of large valley floor moraine dams. We place these drainage events in the context of Late Quaternary meltwater pathways associated with advance/retreat of the Patagonian Ice Sheet and early human occupation across the region. Although broad patterns of ice retreat and lake formation may be similar across Patagonia, driven by Southern Hemisphere palaeoclimate, regional topographic settings likely resulted in spatial and temporal heterogeneity of Atlantic-Pacific drainage reorganisation across southernmost South America.

1. Introduction

During deglaciation of Quaternary ice sheets, modification of glaciofluvial drainage systems may occur, and in suitable geomorphological settings, proglacial lakes can develop as glaciers recede (Carrivick and Tweed, 2013; Dietrich et al., 2017; Palmer and Lowe, 2017). Large proglacial lake systems can store significant volumes of freshwater that can be released over very short time-scales, for example, by glacial lake outburst floods (GLOFs) (Baker, 2009), with the potential to trigger freshwater forcing of abrupt climate change through influences on oceanic circulation (Condron and Winsor, 2012). The deglaciation of the Patagonian Ice Sheet (PIS) (Fig. 1) was associated with the growth, evolution, and drainage of large proglacial lakes, and the continental-scale reorganisation of meltwater drainage from the Atlantic to Pacific Ocean (Caldenius, 1932; Turner et al., 2005; Bell, 2008; García et al., 2014). In central Patagonia (46–48°S), Glasser et al. (2016) employed a freshwater hosing experiment to suggest that drainage reversal events could have altered regional climate change by initiating a negative salinity anomaly that impacted oceanic vertical mixing. However, the exact configuration, timing and drainage routes of palaeolake systems in this region remains equivocal, as suggested by a series of competing lake evolution models (Turner et al., 2005; Hein et al., 2010; Bourgois et al., 2016; Glasser et al., 2016; Martinod et al., 2016), that

* Corresponding author.
E-mail address: Varyl.Thorndycraft@rhul.ac.uk (V.R. Thorndycraft).

https://doi.org/10.1016/j.quascirev.2018.10.036

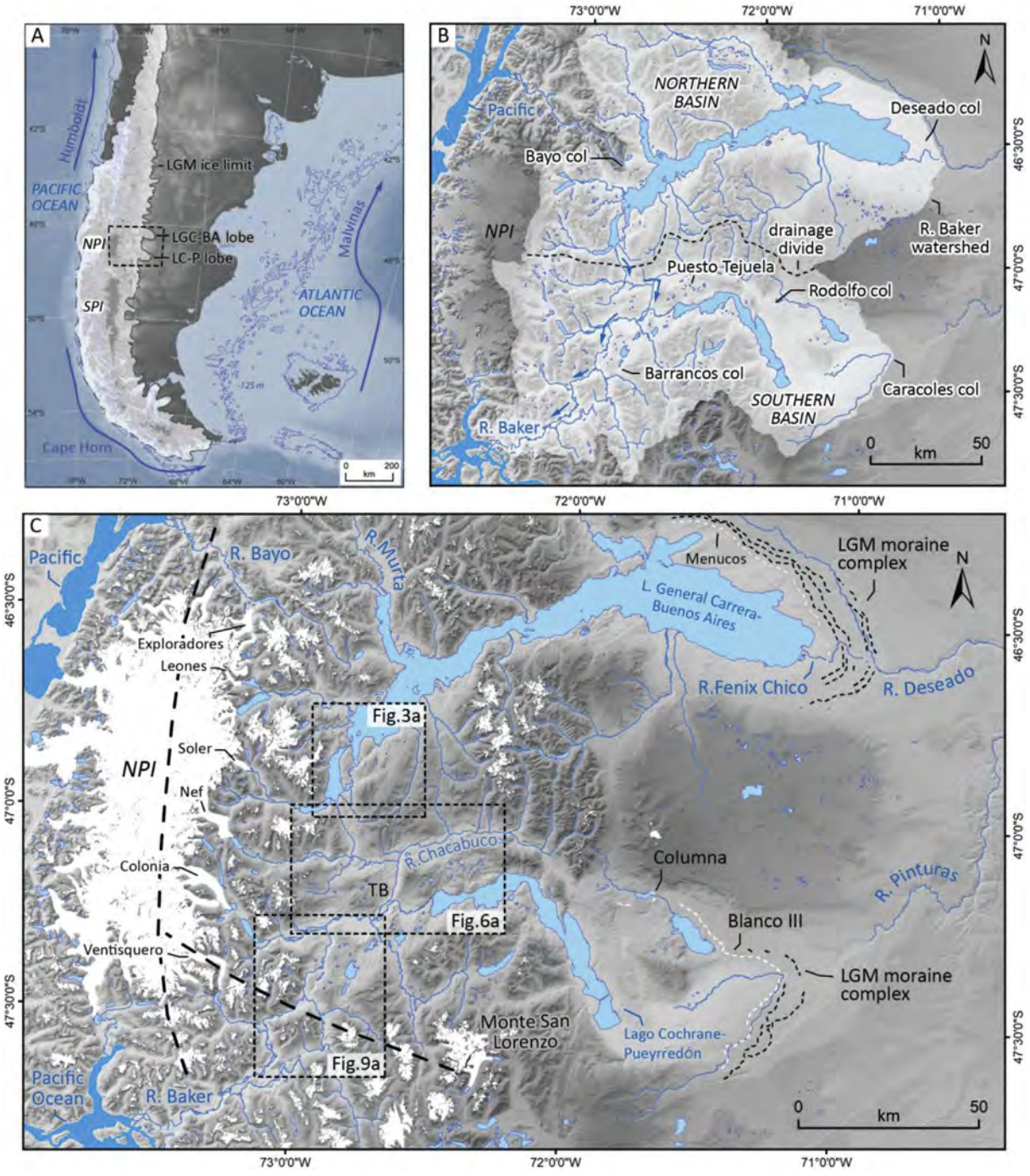

Fig. 1. (a). The study area in southern South America with the LGM ice limit of the former Patagonian Ice Sheet (PIS) (Bendle et al., 2017a) and principal ocean currents shown. (b) The Río Baker catchment, divided into northern and southern basins as used in the text. Blue arrows indicate river flow direction. Also shown are the major palaeolake outflow cols discussed in the text. (c) Regional map showing the spatial context of the main field study areas to the Northern Patagonian Icefield (NPI) and the basins of Lago General Carrera/Buenos Aires (LGC-BA) and Lago Cochrane/Puerreydón (LC-P), the two lakes hypothesised to join through the Baker Valley in the Tamango Basin (TB) sector. Contemporary glaciers (Randolph Glacier Inventory) are shown in white, highlighting both the NPI and Monte San Lorenzo (MSL) ice cap. Also shown are the LGM limits (dotted lines) associated with the main eastward flowing ice-lobes of the PIS, and the LGM ice divides (black dashed lines) from Hubbard et al. (2005). Dates from the youngest moraines (white dotted line) are used in our geochronological review.

are unable to reconcile all available geochronological data (Fig. 2).

Well-constrained palaeolake extents and timings are an essential foundation for robust palaeogeographic reconstructions and climatic inferences from proposed freshwater forcing events, as demonstrated by Breckenridge (2015) for the drainage of glacial Lake Agassiz in North America. Systematic geomorphological analyses, which facilitate the quantification of regional isostatic history, are imperative in this goal. To this end Bendle et al. (2017a) produced a detailed dataset (>35,000 landforms) of regional glacial and palaeolake geomorphology at a higher resolution than previous mapping (e.g. Glasser et al., 2008; Glasser and Jansson, 2008). This work identified previously unidentified ice margin landforms

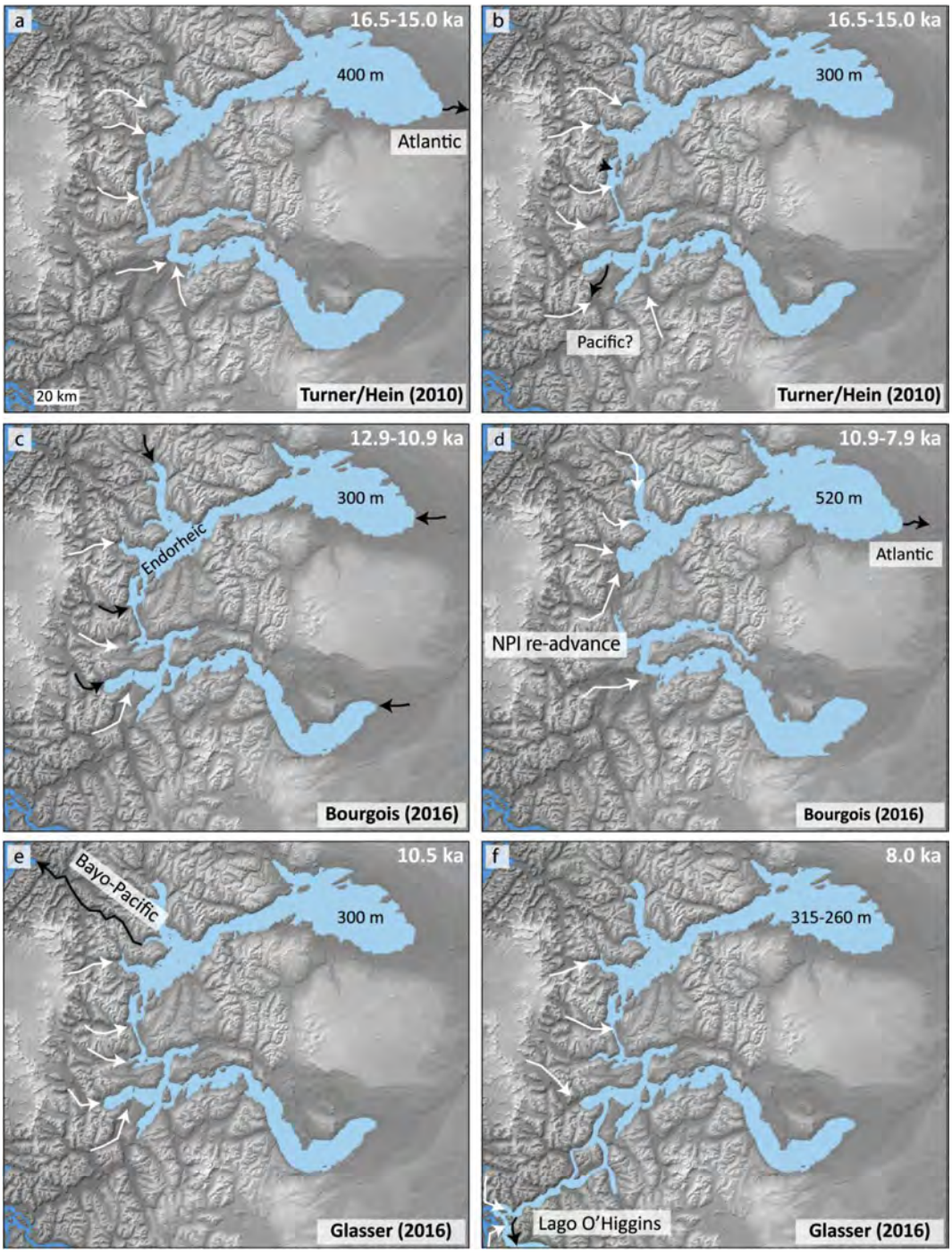

Fig. 2. Summary maps illustrating the main stages of published palaeolake evolution models demonstrating a range of interpretations for the formation and drainage of Lago Chalenko. White arrows indicate major glacier flow pathways, black arrows indicate lake drainage routes. (a) The upper unified lake at the ~400 masl level (Hein et al., 2010, cf. Turner et al., 2005). (b) The lower unified lake at the~ 300 masl level, with a hypothesised but unidentified drainage pathway to the Pacific (Hein et al., 2010). (c) An endhoreic drainage stage proposed by Bourgois et al. (2016). (d) Holocene transgression of LGC/BA to ~520 masl (Bourgois et al., 2016). (e) The lower unified lake level at ~300 masl, with Pacific drainage to the north of the Northern Patagonian Icefield via the Bayo Valley (Glasser et al., 2016). (f) A unified lower lake at ~260 masl dammed with a drainage pathway via Lago O'Higgins/San Martin (Glasser et al., 2016), a lake of the Southern Patagonian Icefield region (shown on Fig. 16).

and lake level evidence making a new reconstruction timely.

The aim of this paper is to evaluate existing models of palaeolake evolution and Atlantic-Pacific drainage reorganisation in the sector 46–48°S. This aim was achieved by firstly targeting new field mapping to better characterise palaeolake geomorphology in areas central to understanding lake evolution. The Baker valley (Fig. 1b), for example, is critical to understanding the potential coalescing of former lake systems (Mercer, 1976; Turner et al., 2005), as well as the opening of a westwards drainage pathway to the Pacific, however to date there is limited fluvial palaeohydrology research from the basin. Secondly, an altitudinal-based assessment of published geochronology was undertaken to evaluate potential timings for ice-margin and palaeolake levels and extent. Existing geochronological reviews have focused on the planform

distribution of available dates (e.g. Rebassa et al., 2011; Mendelova et al., 2017), overlooking important geomorphological information on sample altitude and, therefore, landform relationships with palaeolake elevations. Additionally, we targeted new cosmogenic nuclide exposure (CND) ages from a key ice margin blocking drainage of Lago General Carrera/Buenos Aires (Fig. 1). Thirdly, to provide constraints on palaeolake extent, post-glacial isostatic rebound was quantified using a systematic histogram-based analysis (*cf.* Breckenridge, 2013) of the regional shoreline mapping dataset (Bendle et al., 2017a). This represents the first assessment of glacio-isostatic adjustment and shoreline distance-elevation relationships at the regional scale, and builds on previous reconstructions based on spot-height measurements obtained from raised lacustrine deltas (Turner et al., 2005; Glasser et al., 2016; Martinod et al., 2016).

More broadly the study will have relevance for: a) understanding long-term Quaternary landscape development and the position of the continental drainage divide located to the east of the Andean Cordillera (associated with glacial landforms); and b) understanding the Late Quaternary palaeohydrology of Atlantic-Pacific drainage reversals and lake level drainage events in relation to early human occupation (~14.5-11.5 ka) in Patagonia (Dillehay et al., 2015; Borrero, 2015).

2. Regional context

2.1. Geomorphological context

The study area (Fig. 1) is centered on the Northern Patagonian Icefield region (46–48°S) of the Patagonian Cordillera, encompassing the Río Baker catchment (Fig. 1b). Extensive latero-frontal moraine complexes demonstrate that the Buenos Aires and Puerreydón ice-lobes of the former Patagonian Ice-sheet advanced to the Argentinean steppe (Caldenius, 1932; Glasser and Jansson, 2005; Bendle et al., 2017a) over 150 km east of contemporary ice limits, blocking the westwards drainage of rivers and causing continental drainage to flow eastward to the Atlantic Ocean (Caldenius, 1932; Turner et al., 2005). The local Last Glacial Maximum (lLGM) limits of the Buenos Aires and Puerreydón ice-lobes have been dated to ~20–23 ka (Douglass et al., 2006) ~20–27 ka (Hein et al., 2010) respectively, based on CND ages of moraine boulders. Glaciological modelling suggested two major lLGM ice divides (Hubbard et al., 2005) – a north-south divide aligned along the Andean Cordillera, and a west-east divide connecting Monte San Lorenzo to the Andean Cordillera across the Baker valley (Fig. 1c).

Using a varve record (FCMC17) constrained by the Ho tephra of Cerro Hudson, Bendle et al. (2017b) dated the onset of deglaciation from the Fenix I moraine of the Buenos Aires lobe to ~18.1 ± 0.21 cal ka BP, with a subsequent acceleration in ice retreat from the Menucos moraine at ~17.7 ± 0.12. These data support published CND ages from moraines in the region: Douglass et al. (2006) dated the Fenix I moraine to 18.7 ± 1.7 ka and the Menucos moraine to 17.5 ± 1.3 ka (both recalculated ages presented in Bendle et al., 2017b). CND ages from the Puerreydón lobe are broadly equivalent in timing, within errors (Hein et al., 2010). The subsequent thinning and recession of regional ice lobes (Glasser et al., 2012; Boex et al., 2013) enabled the formation and growth of large proglacial lake systems (Turner et al., 2005; Bell, 2008). The culmination of this recessional phase is marked by moraine ridges formed around the morpho-tectonic boundary of the Patagonian Cordillera, to the west of the Tamango Basin (TB, Fig. 1c), which indicate a phase of glacier stabilisation, or re-advance. Glasser et al. (2012) dated this re-advance to the period 12.8-11 ka, coincident in time with the Northern Hemisphere Younger Dryas interval, and interpreted this as the maximum ice limit post-lLGM. However, earlier ages dating to the Antarctic Cold Reversal (ACR), defined as 14.5-12.8 ka (Pedro et al., 2016), were obtained from ice margins of the Colonia valley of the Northern Patagonian Icefield (Nimick et al., 2016) and the Tranquilo valley of Monte San Lorenzo (Sagredo et al., 2018). ACR readvances have also been reconstructed from the Southern Patagonia Icefield (e.g. Moreno et al., 2009; Putnam et al., 2010; Sagredo et al., 2011, García et al., 2012). Based on climate-modelling simulations, Pedro et al. (2016) suggest that the ACR cooling signal extended as far north as 40°S, so likely encompassed the study region. The ice-sheet model of Hubbard et al. (2005) for the North Patagonian Icefield, while driven by the Vostok ice-core record that displays an ACR signal, suggests that a stabilisation, and even small increase in ice sheet volume, may have resulted in response to the ACR. To summarise, the largest post-lLGM readvance likely occurred during the ACR.

The major morphological feature of present-day regional drainage is the Río Baker catchment (Fig. 1b), which drains an area of ~27,000 km^2 (Dussaillant et al., 2012). The main valley flows north to south cutting across the west-east trending valleys occupied by outlet glaciers during Quaternary glaciations. The Río Baker is fed by large transboundary lakes in two major basins: Lago General Carrera/Buenos Aires in the northern basin; and Lago Cochrane/Puerreydón in the southern basin (Fig. 1b). The drainage of both lakes is reversed relative to the flow pathways of the former ice-lobes (Fig. 1b).

2.2. Palaeolake evolution

Fig. 2 summarises the main palaeolake evolution models for the region. The models are underpinned by independent geochronological datasets (Table SM1). Turner et al. (2005) relied primarily on basal radiocarbon dates from small kettle holes to constrain ice positions and/or lake level changes. Hein et al. (2010) and Bourgois et al. (2016) used CND ages from glacial and ice-rafted boulders to infer the timings of lake levels. Glasser et al. (2016) used optically stimulated luminescence (OSL) to directly date shoreline deposits. In all models, during initial retreat from lLGM extent, lakes continued to drain eastwards to the Atlantic Ocean through the Deseado and Pinturas rivers (Fig. 1c). Glasser et al. (2016) however, inferred a higher lake level in the northern basin (not shown in Fig. 2) of 480–550 m above sea level (m asl). The geomorphology of raised deltas and palaeoshorelines provide evidence for subsequent lake level falls (Bell, 2008), in response to retreating ice-dam positions (Turner et al., 2005; Glasser et al., 2016). The models also have in common the reconstruction of a large unified lake (Turner et al., 2005; Hein et al., 2010), formed when the northern and southern basins joined through the Baker valley following retreat of the Soler and Nef glaciers (Fig. 1c). This lake was named Glacial Lake Patagonia Ice Sheet by Glasser et al. (2016), however given the number of unified glacial lakes throughout Patagonia (e.g. Sagredo et al., 2011; García et al., 2014) we use the name Lago Chalenko, the indigenous name for Lago General Carrera/Buenos Aires.

Differences between the models relate to reconstructions of the position of lake drainage outlets and the timing of lake unification. In the Turner-Hein model, Lago Chalenko formed at an upper ~400–440 m asl level (Fig. 2a) by 16 ka, with a lower ~300–340 m lake (Fig. 1b) established after drainage switched from the Atlantic to Pacific. Final lake drainage through the Baker valley happened by 12.8 ka (Mercer, 1976; Turner et al., 2005) or earlier (by 15.5 ka) depending on a possible, but unidentified, Baker valley drainage pathway (Fig. 2b, Hein et al., 2010). Bourgois et al. (2016) suggested a multi-phase lake evolution model that includes an endorheic stage (Fig. 2c), caused by a reduction in regional precipitation, before lake drainage and a subsequent Holocene (10.9-7.9 ka)

transgression phase up to 520 m asl (Fig. 2d), an interpretation questioned by Martinod et al. (2016) who suggest the higher elevation deltas relate to smaller ice-marginal lakes. Alternatively, Glasser et al. (2016) hypothesised a first Atlantic-Pacific drainage reversal through the Bayo Valley by 10.5 ka (Fig. 2e) before the formation of a spatially larger unified lake at 315-260 m asl, dammed by a still coalesced Patagonian Ice-sheet in the fjords at the mouth of the Río Baker (Fig. 2f). In this scenario outflow drainage was proposed via Lago O'Higgins, a proglacial lake of the Southern Patagonian Icefield. Separation of the north and south icefields occurred by ca 8 ka allowing final lake drainage to contemporary levels. The differences between the models (Fig. 2) primarily reflect the independent geochronological datasets used, hence they are not able to reconcile all available dates. Consequently, for example, there is a ~5000-year gap between the oldest (15.5 ka) and youngest (10.5 ka) age for the timing of the first Atlantic-Pacific drainage reversal (Mendelova et al., 2017).

3. Materials and methods

3.1. Geomorphological mapping

This paper uses data from a previously published geomorphological map of the 46–48 °S region of the former Patagonian Ice-sheet (Bendle et al., 2017a). Glacial and lacustrine landforms were mapped in ArcGIS v10.1 from ESRI™ *World Imagery* datasets (mainly ~1 m DigitalGlobe and GeoEye IKONOS imagery), GoogleEarthPro™, with localised field verification. Additionally, we present new field mapping from three sectors: (1) the Lago General Carrera outflow at Lago Bertrand (upper box, Fig. 1c); (2) the Chacabuco-Cochrane sector of the Baker and Cochrane valleys (middle box, Fig. 1c); and (3) the Colonia-Barrancos sector (lower box, Fig. 1c). Sectors 1–2 are critical for understanding the blocking and opening of the upper Baker valley and the linking of palaeolakes between the northern and southern basins. Sector 3 is relevant to the blocking and opening of Pacific drainage through the lower Baker valley. Landforms in the Baker-Colonia sector were mapped using a differential GPS (Leica), and hand held GPS units were used in the other sectors. In total we carried out 7 field campaigns in these study areas between April 2011 and October 2017.

3.2. Proglacial lake reconstruction and glacio-isostasy

Using palaeoshoreline indicators mapped in Bendle et al. (2017a), we analysed shoreline distance-elevation relationships to quantify glacio-isostatic uplift of separate palaeolake levels, adopting comparable methods to those outlined in Breckenridge (2013, 2015). Mapped shoreline features included wave-cut scarps, terraces, raised deltas and isthmuses. Individual shoreline features were digitised by drawing a line along the break slope of a former waterline. These polylines were converted into points at 30 m spacing, and the elevation of each point extracted from an ASTER G-DEM (20 m vertical and 30 m horizontal resolution (95% confidence); *cf.* ASTER G-DEM Validation Team, 2011). To visualise spatial patterns in shoreline elevation, a surface was interpolated from the point elevations using a Natural Neighbour function. Using this raster, rebound isobases were constructed manually as distance contours at 10 km intervals, perpendicular to the direction of maximum uplift. The 0-km isobase was defined by the easternmost extent of shoreline evidence, and intersects the former Río Deseado outflow (~398 m asl) at Río Fenix Chico. For every shoreline point, distance along the direction of maximum uplift was then extracted from the rebound surface, plotted against shoreline elevation, and palaeo-waterlines correlated.

Assessments of the isobase surface were made using an iterative histogram analysis (cf. Breckenridge, 2013), to evaluate the fit of shoreline elevations to a best-fit regression line. In analysing palaeoshorelines of Lake Agassiz, Breckenridge (2013) used 3 m resolution LiDAR data. The ASTER G-DEM has a comparatively low vertical resolution (20 m), but represents the highest resolution topographic dataset available to the authors. Beginning with the best-developed shoreline level (a ~300–350 m asl level in the Northern Basin that we term the Bayo level), the complete point dataset was split along the former lake centre-line, and the shoreline point data divided into northern and southern shoreline datasets. Subsequently, a 2nd-order polynomial regression line was fitted to the most densely populated dataset to define a modelled shoreline that describes shoreline elevation as a function of distance (cf. Breckenridge, 2013, 2015). Using the polynomial regression line, histograms were then created for each side of the basin. Using 1 m-wide x-axis bins for variations in the y-intercept (shoreline elevation) of the regression line, the y-axis plots the number of points that fall within 1/2 m of the shoreline equation. The fit of the isobase surface was assessed by visually comparing the output histograms. Where there were slight offsets in the alignment of northern and southern shoreline histograms, isobases were re-contoured through repeated iterations, and the regression analysis reapplied until histograms precisely overlapped and a final set of isobases was achieved. Once the isobase surface had been validated for the best-developed shoreline level, the histogram analysis was extended to all other palaeolake levels in the northern (Lago General Carrera/Buenos Aires) and southern (Lago Cochrane/Puerreydón and Chacabuco) basins. The full dataset is available at https://doi.org/https://doi.org/10.17637/rh.6480530 (Bendle, 2018).

3.3. Geochronology

3.3.1. Cosmogenic nuclide exposure dating (CND) of morainic boulders

A moraine complex located on the western valley margin above Lago Bertrand and the contemporary Lago General Carrera outflow (cf. Bendle et al., 2017a) was targeted for CND sampling because ice here, sourced from the Soler Glacier, would have blocked drainage from the northern basin to the Baker valley (Figs. 1 and 3a). The timing of this ice margin is, therefore, critical for understanding the timing of palaeolake evolution and the formation of Lago Chalenko through the Baker valley.

Samples for ^{10}Be exposure-age dating (Table 1a) were taken from boulders with b-axes >1 m, perched on moraine crests (cf. Putkonen and Swanson, 2003; Heyman et al., 2016), and exhibiting evidence of glacial transport, such as rounded edges and faceting (Figs. 4b and 4c). Sample details and results are presented in Table 1a. Rock samples were collected following standard procedures (Gosse and Phillips, 2001; Cockburn and Summerfield, 2004; Balco, 2011; Darvill, 2013). Samples (<5 cm thick and weighing >1 kg) were taken using a hammer and chisel from the centre of the flat top surface of the boulders, away from cracks, edges and joints. In total 6 boulders were analysed from the Bertrand moraine complex to provide sufficient samples to allow the exclusion of anomalous results arising from inheritance, rolling, exhumation or burial (Putkonen and Swanson, 2003; Cockburn and Summerfield, 2004).

Ages were calculated using the CRONUS-Earth online calculator, version 2.3 (Balco et al., 2008). We used the local Patagonian production rate (50°S) from Kaplan et al. (2011). Ages are presented with the Lal/Stone time-dependent scaling protocol scheme (Lm) (Lal, 1991; Stone, 2000). We used a rock density of 2.7 g/cm^3 and the 07KNSTD AMS standard for normalisation (Nishiizumi et al., 2007).

Erosion rates are poorly constrained regionally so we applied an

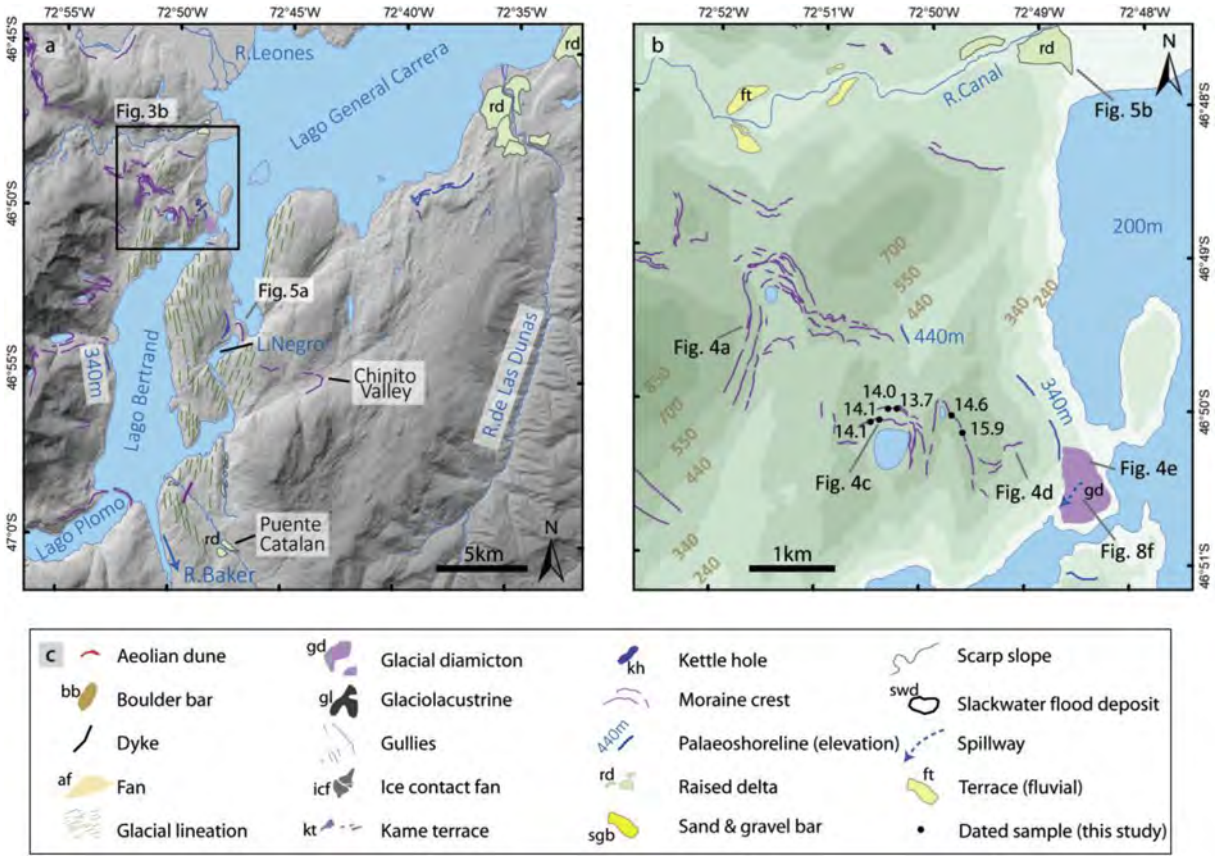

Fig. 3. (a). Geomorphological map of the Lago Bertrand sector illustrating moraine crests at the col between the Bertrand and Canal Valleys and in the Chinito valley. Raised deltas are also illustrated (cf. Bendle et al., 2017a). (b). Map of the moraine complex adjacent to the LGC/BA outflow into Lago Bertrand, with CND ages of sampled boulders illustrated. Photo locations for Figs. 4 and 8f are shown. (c). Legend for the geomorphological maps presented in Figs. 3, 6 and 9.

Table 1
Summary geochronological information. a) CND samples from the Lago Bertrand moraine site; and b) OSL sample of a loess deposit.

a) Cosmogenic dating

Sample	Latitude	Longitude	Elevation (m asl)	Sample thickness (cm)	Shielding factor	^{9}Be spike (μg)	Total Qtz (g)	Be cathode	^{10}Be/^{9}Be (x10^{-15})	^{10}Be[a] (x10^{4} atom/g)	^{10}Be age[b] (ka) 0 mm/a	^{10}Be age[b] (ka) 1 mm/a
LB-15-2	−46.8374	−72.8403	554	2	0.9954	225.83	11.42	b11001	73.1 ± 2.2	9.21 ± 0.33	14.0 ± 0.8 (0.5)	14.2 ± 0.8
LB-15-3	−46.8358	−72.8403	577	5	0.9982	225.83	22.74	b11002	142.6 ± 4.2	9.24 ± 0.31	14.1 ± 0.7 (0.5)	14.3 ± 0.8
LB-15-4	−46.8358	−72.8433	575	4	0.9982	225.58	17.87	b11003	113.8 ± 3.2	9.32 ± 0.31	14.1 ± 0.7 (0.5)	14.3 ± 0.8
LB-15-5	−46.8340	−72.8405	566	3.5	0.9954	225.83	10.40	b11005	65.0 ± 2.1	8.94 ± 0.35	13.7 ± 0.8 (0.5)	13.9 ± 0.8
LB-15-6	−46.8340	−72.8293	601	1.5	0.9970	224.82	21.14	b11006	144.8 ± 4.3	10.1 ± 0.34	14.6 ± 0.8 (0.5)	14.8 ± 0.8
LB-15-7	−46.8340	−72.8276	630	3.5	0.9902	225.24	9.32	b11007	70.9 ± 2.1	10.9 ± 0.39	15.9 ± 0.9 (0.6)	16.1 ± 0.8

b) Optically Stimulated Luminescence dating

Sample	Latitude	Longitude	Elevation (m asl)	Sample depth (m)	Dose rate (Gy/ka)	Equivalent dose	Water (%)	^{40}K (Bq/kg)	^{232}Th (Bq/kg)	^{232}U (Bq/kg)	Age
CL1256	−47.130	−72.689	190	0.70	2.67 ± 0.12	20.8 ± 0.9	15	381 ± 37	39 ± 2	25 ± 2	7.8 ± 0.5

Internal uncertainties (±1σ) shown in parentheses reflect analytical uncertainties on sample processing and ^{10}Be measurements. External uncertainties (±1σ) incorporate, in addition, uncertainties related to calibration (production rate) and scaling procedure.

[a] Normalised to the '07KNSTD' standardization of Nishiizumi et al. (2007) and corrected for a procedural chemistry background of 50751 ± 11188 ^{10}Be atoms. Uncertainties (±1σ) include all known sources of analytical error.

[b] Calculated using version 2.3 of the online exposure age calculators formerly known as the CRONUS-Earth online exposure age calculators (Balco et al., 2008) with the production rate of Kaplan et al., (2011) as derived from the ICE-D database (http://calibration.ice-d.org/).

Fig. 4. Photographs from the Bertrand moraine complex. (a) View to the north from a lateral moraine at ~600 m asl dipping down to the ice margin sat on the col separating the Bertrand and Canal valleys. (b) Granite boulder (BM-15.6) sampled for CND, with the lateral moraine in Fig. 4a highlighted. (c) Granite boulder (BM-15.3) sampled for CND, with LGC-BA in the background. (d) Lateral moraine dipping towards LGC-BA, with the dashed line showing the top of a cliff edge that marks the limit of the moraine. (e) View of the northerly margin of glacial diamicton capped by a boulder field at the contemporary outflow of LGC-BA. The photo is taken from a palaeoshoreline at ~340 m asl. (f) View from the Bertrand moraine complex towards the Plomo moraine, dated to 10.6 ka (Glasser et al., 2012), representing an ice limit of the Soler Glacier following opening of the Baker valley. Ice flow was towards the camera showing how ice at the Bertrand moraines would have blocked the Baker valley. Photos by V.R. Thorndycraft.

erosion rate of 0 mm/kyr, but also provide ages with 1 mm/kyr erosion rates for comparison (Table 1a). Erosion rate leads to little difference on boulder exposure ages within the timescale of this study (see Glasser et al., 2012) so choice of erosion rate is unlikely to affect the findings of the paper. The difference in calculated age is smaller than the calculated uncertainties at this timescale. We provide both the internal uncertainties, determined by the error in nuclide concentration, and external uncertainties relating to production rate (Balco et al., 2008). We used the external (total) uncertainty to compare the Bertrand moraine ages with other published ages (Section 3.3.3) including those using different methods (e.g. radiocarbon).

3.3.2. *Optically stimulated luminescence (OSL) dating*

Samples for OSL (Table 1b) were taken from fluvioglacial sands and aeolian silts to constrain the timing of palaeodrainage events, however only the one sample taken from a loess deposit was dated successfully (Table 1b). This is likely because the sampled fluvioglacial sands were taken from high magnitude flood deposits (see example sedimentary descriptions in Section 4.1.2), and so are insufficiently bleached compared to the outwash and beach sediments dated by Smedley et al. (2016) and Glasser et al. (2016), respectively. For the loess sample, the single aliquot regenerative dose (SAR) protocol was used, applied on 24 quartz multi-grain aliquots (~30 grains each) measured using blue OSL. The equivalent dose was estimated using the Central Age Model (Galbraith

et al., 1999) on the distribution, excluding three outliers (i.e. dose values out of 1.5 times the interquartile range). Dose rate has been calculated from the concentration of radionuclides within the sample, measured with high resolution gamma spectroscopy. Total annual dose rate and derived age have been calculated using DRAC v1.2 (Durcan et al., 2015).

3.3.3. Altitudinal-based review of published geochronology

We reviewed published ages from samples relevant to understanding the timing of deglaciation and palaeolake evolution (see Supplementary Materials, SM1). Our review was focused on sample altitude, to provide a topocentric dataset to examine alongside our analysis of shoreline isostasy (Section 3.2.4) and allow a more complete assessment of palaeolake configuration and timings. To date, published ages have mainly been presented on maps (e.g. Glasser et al., 2012) or single axes age-plots. Boex et al. (2013) provide altitudinal information because their focus is on former ice-sheet surface elevation, but the analysis focuses on their own dates in the Chacabuco/Cochrane area, rather than a regional review. Similarly, Glasser et al. (2016) present their OSL dates on an altitudinal plot, but no elevation-based comparison is made to other datasets, nor is isostasy considered in detail.

The geochronology database (Table SM1) includes: (a) CND ages from moraine boulders (Glasser et al., 2012; Bourgois et al., 2016); (b) CND ages from glacial erratics or dropstones with ages relevant to palaeolake levels (Hein et al., 2010; Bourgois et al., 2016); (c) OSL and CND ages from palaeolake landforms (Bourgois et al., 2016; Glasser et al., 2016); and (d) radiocarbon dates from basal organic remains in small kettle holes and closed lake basins (Turner et al., 2005; Villa-Martínez et al., 2012).

To standardise the database, CND ages were recalculated using the same methods outlined in Section 3.3.1, namely the time-dependent scaling scheme (Lm) of Lal (1991) and Stone (2000) was applied, we assumed 0 cm ka^{-1} weathering rates, and the Kaplan et al. (2011) Patagonian production rate was used to calibrate ^{10}Be determinations. Radiocarbon ages were recalibrated in Oxcal v.4.3 (Bronk-Ramsey, 2009) using the SHCal13 calibration curve (Hogg et al., 2013).

3.3.4. Bayesian age modelling

The new dating evidence and geochronological review enabled the development of a Bayesian age model (Bronk-Ramsey, 2009) to analyse the phasing of palaeolake evolution events. This was achieved using a Sequence model in Oxcal 4.3, which allows for the phasing of a known sequence of events (Bronk-Ramsey, 2008). Because model set up depends on our results and geomorphological interpretations, model details (including model code) are presented in the Supplementary Materials (SM2.1). Additionally, a separate P-Sequence age model (Bronk-Ramsey, 2009) was applied to the previously published radiocarbon dates from Lago Augusta (see Fig. 6 for location) to help constrain the timing of a change from glaciolacustrine to organic sedimentation, interpreted as a lake level drop in the Chacabuco valley (Villa-Martínez et al., 2012). In a P-Sequence model sample depth is included and a range of sedimentation rate scenarios can be modelled (SM2.2). Modelled ages (and radiocarbon dates) in the manuscript are reported as cal ka BP.

4. Results and geomorphological interpretations

4.1. Geomorphological mapping

4.1.1. Lago Bertrand sector

In this sector we mapped a moraine complex that extends across multiple valleys situated to the north of the contemporary source of the Río Baker at the Lago Bertrand outflow (Fig. 3a). Remotely sensed mapping (Bendle et al., 2017a) reveals two main moraine locations. The moraines furthest from the Baker source are located to the north of the modern Lago General Carrera outflow, with a second set to the east of Lago Bertrand extends from Lago Negro to the Chinito valley (Fig. 3a). In the field, the moraines located to the north of Lago Bertrand were traced from their eastern limit above Lago General Carrera to an elevation of ~650 m asl above a col (*71°52'33"W 46°49'06"S*, Fig. 3b) dividing the Bertrand and Canal valleys (Fig. 4a). We sampled six boulders for CND (Table 1a; Fig. 3b). Two ages from a moraine crest marking the eastern ice margin were dated to 15.9 ± 0.9 ka and 14.6 ± 0.8 ka (Fig. 4b), and four boulders from moraine crests to the west (e.g. Fig. 4c) cluster around a mean age of 14.1 ka.

The moraine complex terminates above a break of slope (*72°49'03"W 46°50'14"S*) at ~490 m asl (Figs. 3b and 4d), a few hundred metres to the west, and ~200 m in height above, a thick accumulation of glaciogenic diamicton, located on the northern margin of the contemporary Lago General Carrera outflow (Figs. 3b and 4e). This feature was previously described as a moraine by Bourgois et al. (2016), who CND dated a single boulder (17.6 ± 3.8 ka, Table SM.1). We interpret the landform as an ice-contact deposit, possibly a grounding-line fan, formed at the terminus of the Soler Glacier discharging into a lake. Exposures through the Lago Negro moraine (Fig. 5a), at a similar altitude but ~6 km to the southeast (*72°46'58"W 46°53'42"S*, Fig. 3a) are consistent with this interpretation, where north-westerly dipping sand and gravel clinoforms provide evidence for ice-proximal glaciofluvial sediment delivery (e.g. Benn, 1996; Evans et al., 2012) into a lake system dammed to the south by northwards flowing ice. This lake probably existed at an elevation of ~440 m asl, based on the upper elevation of shorelines between the Canal and Bertrand valleys (Fig. 3b), consistent with the elevation of numerous raised deltas (Fig. 3a) mapped further east (Bell, 2008, 2009; Glasser et al., 2016).

A lower shoreline cut into unconsolidated sediments exists at ~340 m asl, and runs along the western margin of Lago Bertrand (Fig. 4f). At the mouth of the Río Canal valley to the north, a raised delta is located at ~340 m asl, and overlies a glaciogenic diamict sequence (Fig. 5b), but no higher elevation delta was mapped. Near Puente Catalan, to the south of Lago Negro, relict deltas are present at ~340 m and ~460 m (Fig. 3a). The ~460 m delta exceeds the previously reported elevation for the upper lake level in the western end of Lago General Carrera/Buenos Aires (e.g. Turner et al., 2005), and the palaeoshoreline mapped in Fig. 3b. We therefore interpret the delta as evidence for a separate ice-marginal lake (see also Section 4.1.2), dammed by the southeast lateral margin of Soler ice occupying the Bertrand valley.

In summary, the landform-sediment assemblages of the western embayment of the northern basin provide evidence for an extensive ice-margin (>0.5 km thick) that existed between 16-13 ka (Table 1; Fig. 4b). The ice was likely sourced from an advanced Soler Glacier, equating to an area of ~160 km^2 of ice blocking the Baker valley at this time and therefore preventing glacial lake linkage between the northern and southern basins. The Lago Plomo moraine (Figs. 3a and 4f), with a mean age 10.7 ka ± 0.4 (Glasser et al., 2012), marks a terminus of the Soler Glacier once drainage was opened from the northern basin into the Baker valley.

4.1.2. Chacabuco-Cochrane sector

In this sector (Fig. 6) we mapped palaeolake landforms including wave-cut shorelines (Fig. 7a–c), raised deltas (Fig. 7e and f) and glaciolacustrine sediments (Fig. 7d), the latter cropping out on both the Chacabuco and Cochrane valley floors. Deltas were field mapped at ~460–470 m asl, ~340–350 m asl (Fig. 6) and ~150 m asl (see Fig. 7e and f). The two uppermost deltas coincide with two

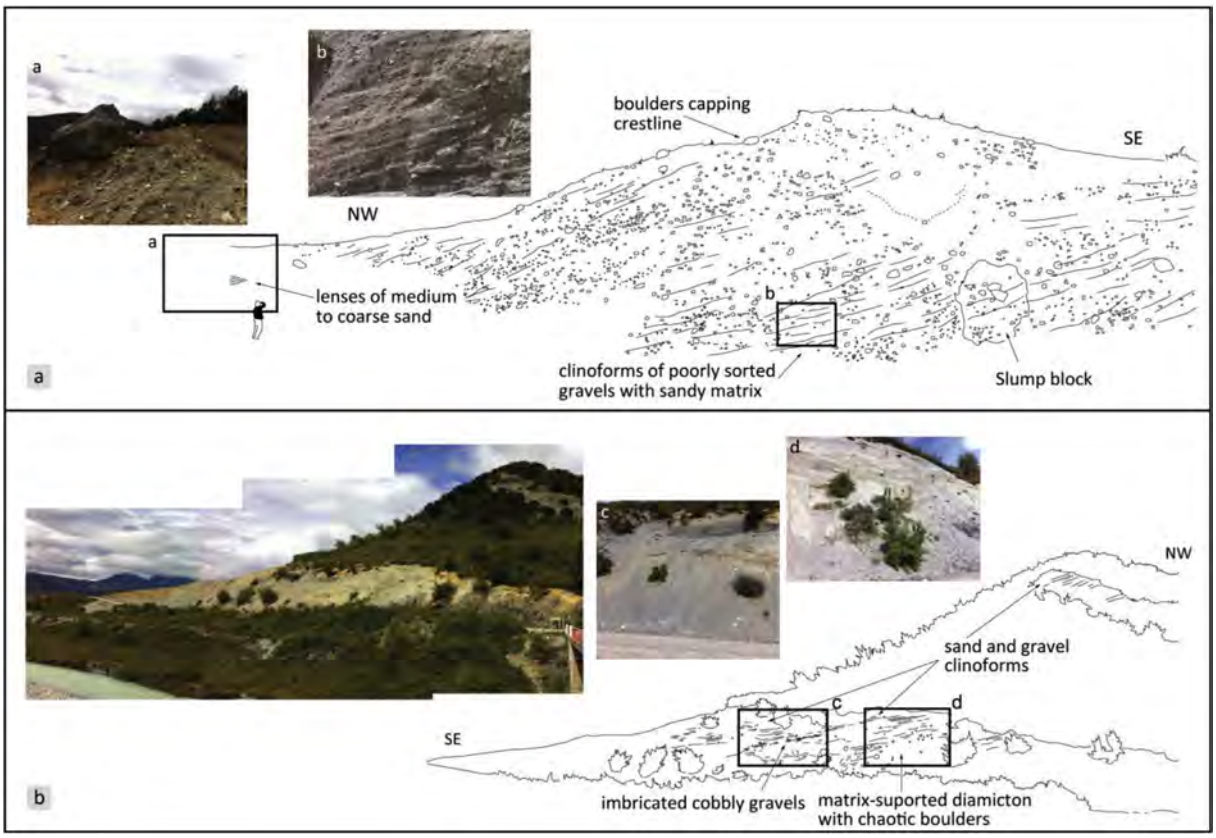

Fig. 5. (a). Sedimentology and field photographs of the Lago Negro moraine (see Fig. 3a for location) showing clinoforms dipping towards LGC-BA. (b). Sedimentology and field photographs of a moraine overlain by a raised delta at the mouth of the Río Canal (see Fig. 3b for location). Photos and sketches by J.M. Bendle.

prominent terrace surfaces interpreted as palaeoshorelines. They feature gently sloping terrace surfaces, usually with boulders, and steeper scarp slopes (e.g. Fig. 7c). Individual segments of shoreline may resemble kame terraces but the key diagnostic evidence is the distance over which the terraces can be traced at similar elevations (e.g. García et al., 2014). The 460–470 m shorelines can be traced in the Baker valley at the Nef-Chacabuco reach (Fig. 7a), along the eastern margin of the Baker Valley ~2 km upstream of the Nef tributary, and in the Maiten Valley (*72°49'38"W 47°10'34"S*, Fig. 6a), indicating that the Nef Glacier had retreated back to (at least) its valley mouth while a ~460–470 m lake level existed. It is likely, therefore, that this lake level extended to the southern ice margin of the Soler Glacier that occupied the Lago Bertrand valley (Section 4.1.1), as demonstrated by the ~460 m asl delta near Puente Catalan (Fig. 3a). It is possible therefore that lake water from the southern basin could have drained via the Soler Glacier to Lago General Carrera/Buenos Aires.

Downstream of the Chacabuco tributary the ~460 m shoreline is coeval with the top of moraine deposits on the eastern valley side (Fig. 7c). Additional shoreline segments were mapped at both ~340–350 and ~460 m asl levels on the northern margin of the Cochrane Valley (Fig. 6c). Here, the ~460 m shoreline is evident above the contemporary Lago Cochrane outflow (Fig. 7b), demonstrating a palaeolake connection between the Cochrane and Chacabuco valleys at this elevation. One delta (Fig. 7e and f), mapped at ~150 m asl (*72°41'28"W 47°17'49"S*, Fig. 6a) Fig. 7e and f) was formed where the Río del Salto enters Valle Grande. Above the delta, on the ice distal face of the Salto moraine, a series of shorelines are visible from the valley floor (Fig. 7f). On the ground the shorelines are more difficult to trace and, where visible, consist of narrow steps. We interpret these as short-lived lake stands during punctuated lake drainage and we note the similarity to previously reported shorelines (Bell, 2008) on the Río del las Dunas deltas (*72°36'15"W 46°46'22"S*, Fig. 3a).

In addition to the palaeolake evidence, fine gravel and sand accumulations, and large boulder-capped bars were mapped (Figs. 6 and 8a-c). A bar-shaped landform, capped with imbricated, metre-sized boulders (Fig. 8a and b), is located in a zone of valley expansion where the Río Baker enters Valle Grande (*72°38'24"W 47°13'21"S* Fig. 6c). Boulder bars are also evident at the western margin of Lago Cochrane (Fig. 8c), ~5–10 m above the contemporary lake outflow, and ~30 m below the surface of glaciolacustrine sediments north of Lago Esmeralda (*72°33'04"W 47°15'12"S*, Fig. 6c). A ~10 m thick exposure of fine gravel and sand deposits in a road cutting (*72°41'22"W 47°07'48"S*, Fig. 6a) consist of cross-bedded fine gravels and sands (Fig. 8d and e) that display climbing ripple structures and rip-up clasts. The deposits are located >50 m above the flood eroded bedrock channel and ~20 m above the valley floor fluvioglacial terrace, so the sedimentology and geomorphic context indicate these deposits are characteristic of high magnitude glacial lake outburst flood (GLOF) events (Carling, 2013). The slackwater deposits are capped by a loess unit that we OSL dated (CL1256) to 7.8 ± 0.5 (Table 1b, Fig. 6b).

The geomorphological implication of the flood evidence is that when the GLOFs occurred there were subaerial conditions in the Baker and Cochrane valleys and so the floods post-date lake drainage from Lago Chalenko. Because a large volume of water would have been required to produce a water depth of >50 m (indicated by the elevation of slackwater deposits above the valley floor) and the energy required to mobilise boulders, we

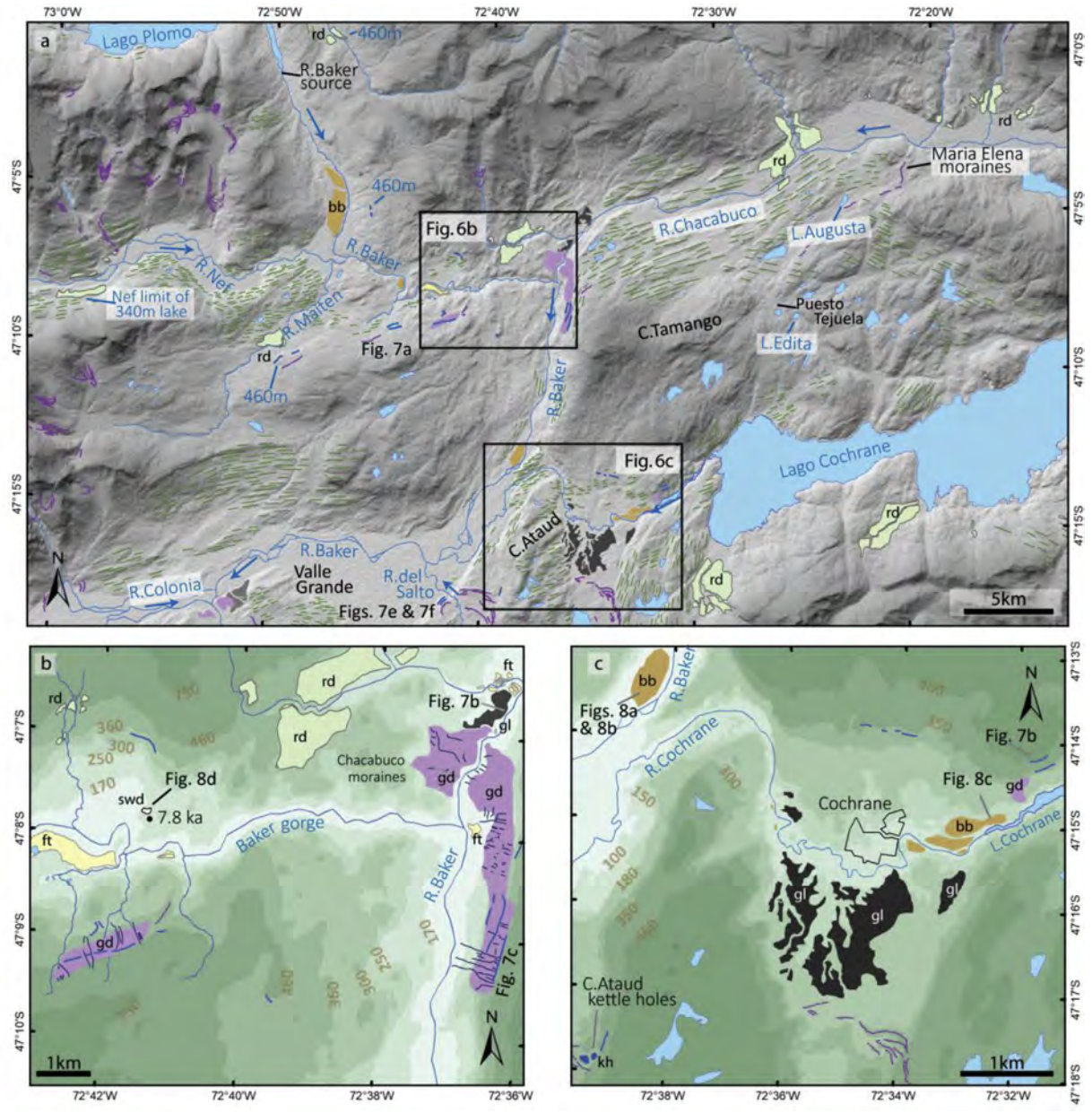

Fig. 6. (a) Geomorphological map of the Chacabuco-Cochrane sector of the Baker valley showing extent of the 460 m asl palaeoshoreline in the Maiten and upper Baker valleys. Blue arrows show river flow directions. (b) Geomorphology of the Baker-Chacabuco confluence sector showing the Chacabuco moraine complex and morph-stratigraphic relationship to palaeoshorelines. Note the 460 m asl palaeoshoreline is located at the top of moraine deposits on the eastern side of the Baker Valley to the south of the confluence. Also shown are slackwater deposits (swd) located upstream of the Baker gorge where GLOF flow hydraulics were controlled by valley narrowing. (c) Geomorphological map of the Cochrane sector showing glaciolacustrine sediments, palaeoshorelines and GLOF bars in the Cochrane and Baker valleys demonstrating two GLOF flow pathways. Note the size of the GLOF bars in relation to Cochrane town. Photo locations for Figs. 7 and 8 are shown. See Fig. 3c for legend.

hypothesise that both Lago General Carrera/Buenos Aires and Lago Cochrane/Puerreydón were dammed by moraines following lake level lowering. In the northern basin, the most likely dam site is the zone of diamicton at the lago General Carrera outflow that we interpreted as a grounding line fan (*72°48'27"W 46°51'33"S* Fig. 3b). The fan surface exhibits a carapace of imbricated boulders (Fig. 8f), providing evidence for southwards flow of water towards the Baker valley. Fluvial incision of the fan surface is indicated by localised terraces (Fig. 8f) and a ~40–50 m high scarp slope that flanks the contemporary lake outflow. In the Southern Basin, morainic deposits on the northern flank of the present-day Lago Cochrane outflow (Fig. 6c) represent the best evidence for a former moraine dam, making a breach at this site the most likely source of the flood.

4.1.3. Colonia-Barrancos sector

The topographic context for the two study sites in this sector is shown in Fig. 9a. The Barrancos sector (Fig. 9b) lies at a watershed at ~420 m asl between the Juncal Valley and the Río Barrancos, a tributary of Río de los Ñadis that feeds into the lower Baker (Fig. 9a). Here, there is evidence for a lake spillway at ~445–470 m asl, with a bedrock cut inner gorge (*72°47'48"W 47°29'05"S,* Fig. 9b and c). For this spillway to function there needed to be ice blocking the lower 420 m asl col (*72°48'40"W 47°29'42"S,* Fig. 9b). We field mapped a segment of moraine either side of Lake A (Fig. 9b). The moraine could not be traced around the lake margin but satellite imagery suggests a submerged segment of this moraine continued across the middle of the lake. We consider the moraine and lake

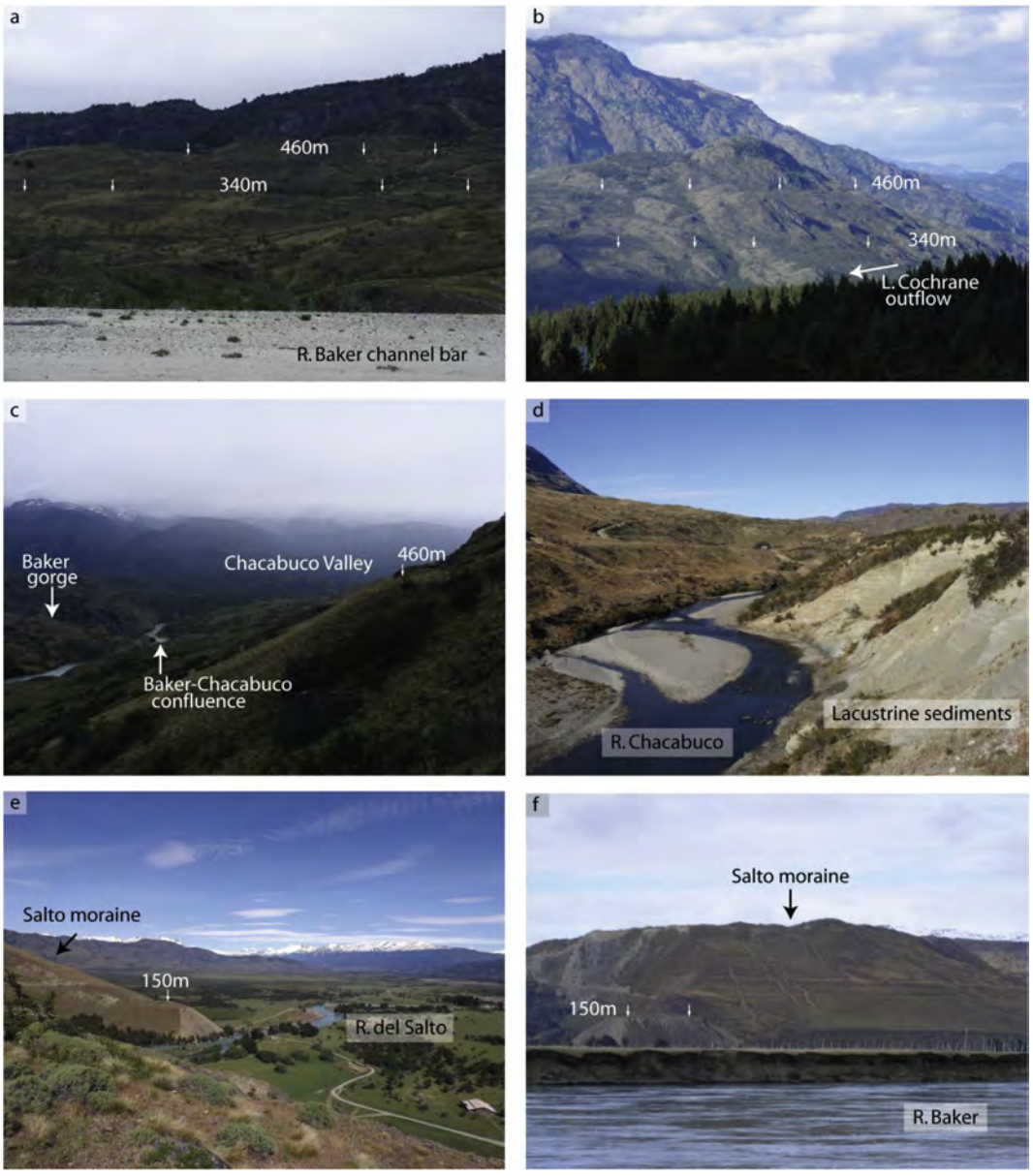

Fig. 7. Photographs of palaeolake landforms. (a) The 460 and 340 m asl shorlines, taken from a channel bar of the Río Baker, downstream of the Maiten valley (Fig. 6a). (b) The 460 and 340 asl shorelines above the Lago Cochrane outflow (Fig. 6c). (c) View upstream towards the Baker-Chacabuco confluence showing the 460 masl shoreline cut into the top of glacial diamicton blanketing the valley side (Fig. 6b). (d) Laminated glaciolacustirne sediments in the lower Chacabuco valley (Fig. 6a). (e) View westwards of a raised delta at ~150 m asl at the exit of Río del Salto in to Valle Grande (Fig. 6a). (f) View of the ~150 m asl raised delta in Valle Grande from the Río Baker. Note the shorelines cut into the ice distal side of the Salto moraine. Photos by V.R. Thorndycraft.

morphology to be analogous to that of a levee and wiel, deep scour pools formed by levee collapse, in fluvial landscapes (e.g. Hudson et al., 2008). Our interpretation, therefore, is that the lake was formed by high energy meltwater flow from the spillway to the north. This suggests the possible rapid collapse of an ice dam at this locality, which caused the downcutting of the inner gorge at the spillway. This interpretation is further supported by the morphology of Lake B which fans out from an apex at the exit of a bedrock channel, and a small terrace preserved on the north margin of the channel exit where flow separation and eddying would occur in response to water flowing in a south easterly direction. Our interpretation, therefore, is that the 460–470 m asl lake level was draining under the Soler Glacier until ice in the Juncal valley had retreated sufficiently to allow the lake to reach the Barrancos spillway, ultimately leading to catastrophic failure and the formation of the landform assemblage mapped in Fig. 9b.

Following the collapse of this ice margin and so abandonment of the valley side spillway, lake drainage into the Barrancos valley may have continued at 420 m asl with drainage over the broad col (Fig. 9b). Evidence for this interpretation is a fan deposit dipping in to the Barrancos valley. To the north of the 420 m asl col is a gullied palaeoshoreline at ~360–370 m asl, which indicates the first stable lake level post-dating abandonment of the Barrancos spillway.

In the Colonia sector (Fig. 9d), a suite of ice-marginal landforms demonstrates a previously unmapped glacial limit. These include a fan shaped deposit at the Colonia-Baker confluence that dips northwards towards the valley floor (*72°51'08"W 47°17'59"S*, Fig. 9d). Exposures through the landform reveal northwesterly-

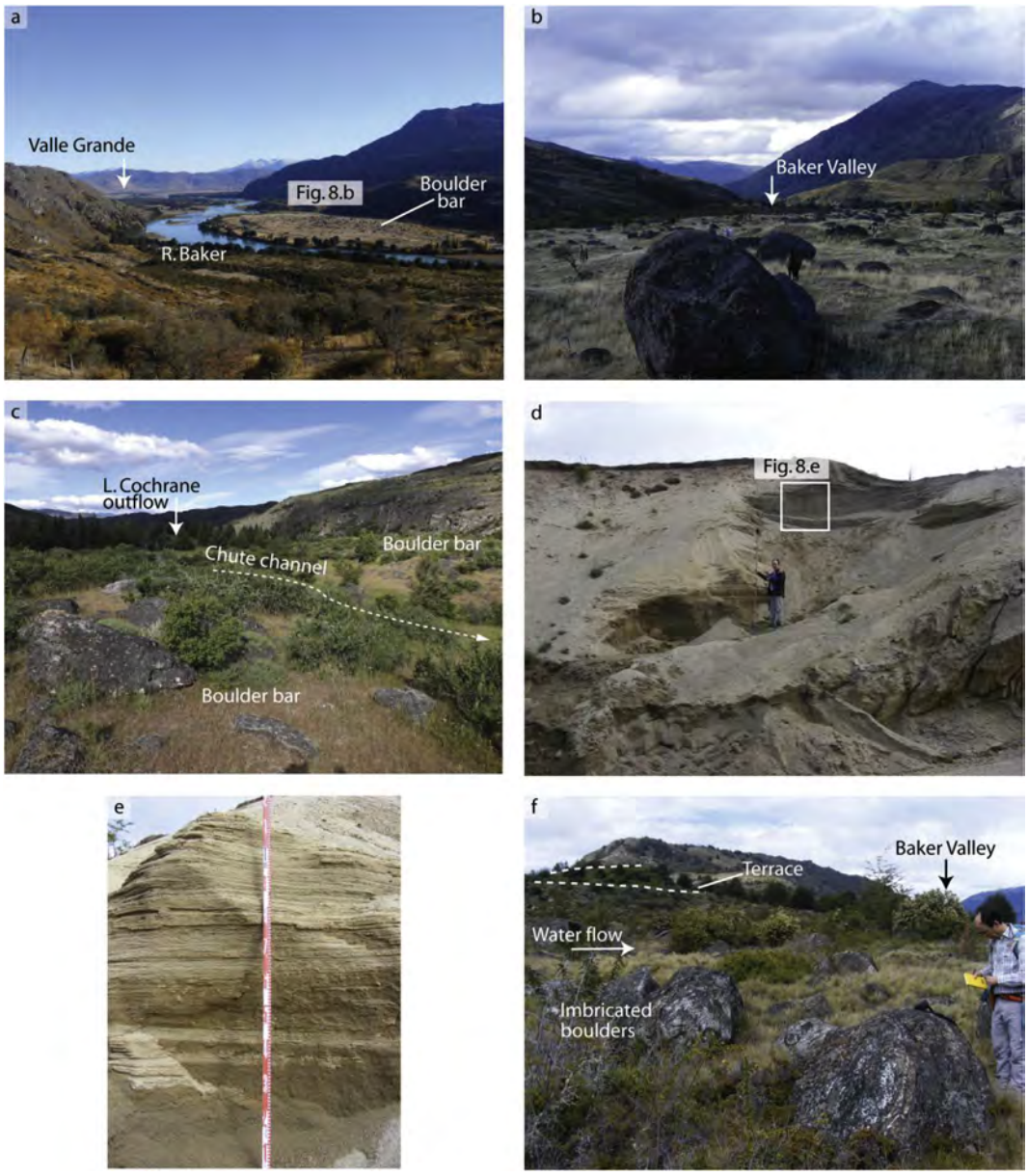

Fig. 8. Photographs of GLOF landforms and sediments. (a) view downstream of a GLOF boulder bar at the zone of valley expansion as the Rio Baker enters Valle Grande (Fig. 6c)). It is likely the boulders are lag-moraine boulders and this could be the site of a former ice margin of the Colonia Glacier. (b) Photo, looking upstream, of flow aligned boulders on top of the boulder bar surface shown in Fig. 8a. Note the horses for scale. (c) View of GLOF boulder bars looking upstream to the Lago Cochrane outflow (Fig. 6c). (d) Slackwater flood deposits exposed in a road cutting ~50 m above the valley floor (Fig. 6a). (e) Cross-stratification in fine gravels and coarse sands at the top of the slackwater flood deposits shown in Fig. 8d. (f) Imbricated boulders at an abandoned spillway on top of the diamicton deposit at the LGC-BA outflow (Fig. 3b). Dipping terrace-like surfaces (one highlighted), also with imbricated boulders, demonstrate incision of the deposit. View is looking to the SW towards the Baker valley. Photos by V.R. Thorndycraft.

dipping gravel beds, which we interpret to reflect ice-proximal subaqueous outwash facies (e.g. Benn, 1996; Evans et al., 2012). The fan apex connects to a series of lateral kame terraces and moraine crests (Fig. 9d) that extend for ~3.5 km to the south. Moraine crests were mapped dipping to the east towards the Juncal valley, where they mark the limit of a second ice lobe (Fig. 9a). Due to forest cover in the Baker valley, it is uncertain whether this ice was sourced from (i) the Cordon Trunco massif (Fig. 9a), which flanks the west of the valley, or (ii) the Ventisquero and/or Río de Los Ñadis valleys to the south (Fig. 9a). Near the Colonia confluence, the valley side moraines and kame terraces are located at ~400 m asl, so this ice margin likely relates to the ~340–370 m asl palaeolake shorelines mapped further upstream (e.g. Fig. 6).

To the west of the Río Baker, a morainic deposit, capped with large boulders, is cut by a channel feature at ~150 m asl (*72°52'45"W 47°18'41"S*, Fig. 9d), an elevation that coincides with the Río del Salto delta in Valle Grande (Fig. 6c). Scarp slopes and terrace surfaces are cut in to the boulder deposit demonstrating incision of the moraine, and a few kilometres downstream, imbricated boulders are present on the valley sides to a maximum elevation of ~115 m asl. The channel and delta indicate a moraine dammed lake, which we name Lago Colonia, at ~120 m asl in Valle Grande. The boulder deposits and terrace scarps, located downstream of the moraine, indicate GLOF drainage of this lake. The multiple terrace scarps eroded in to the moraine deposit were likely formed by subsequent GLOF events from lagos General Carrera/Buenos Aires and

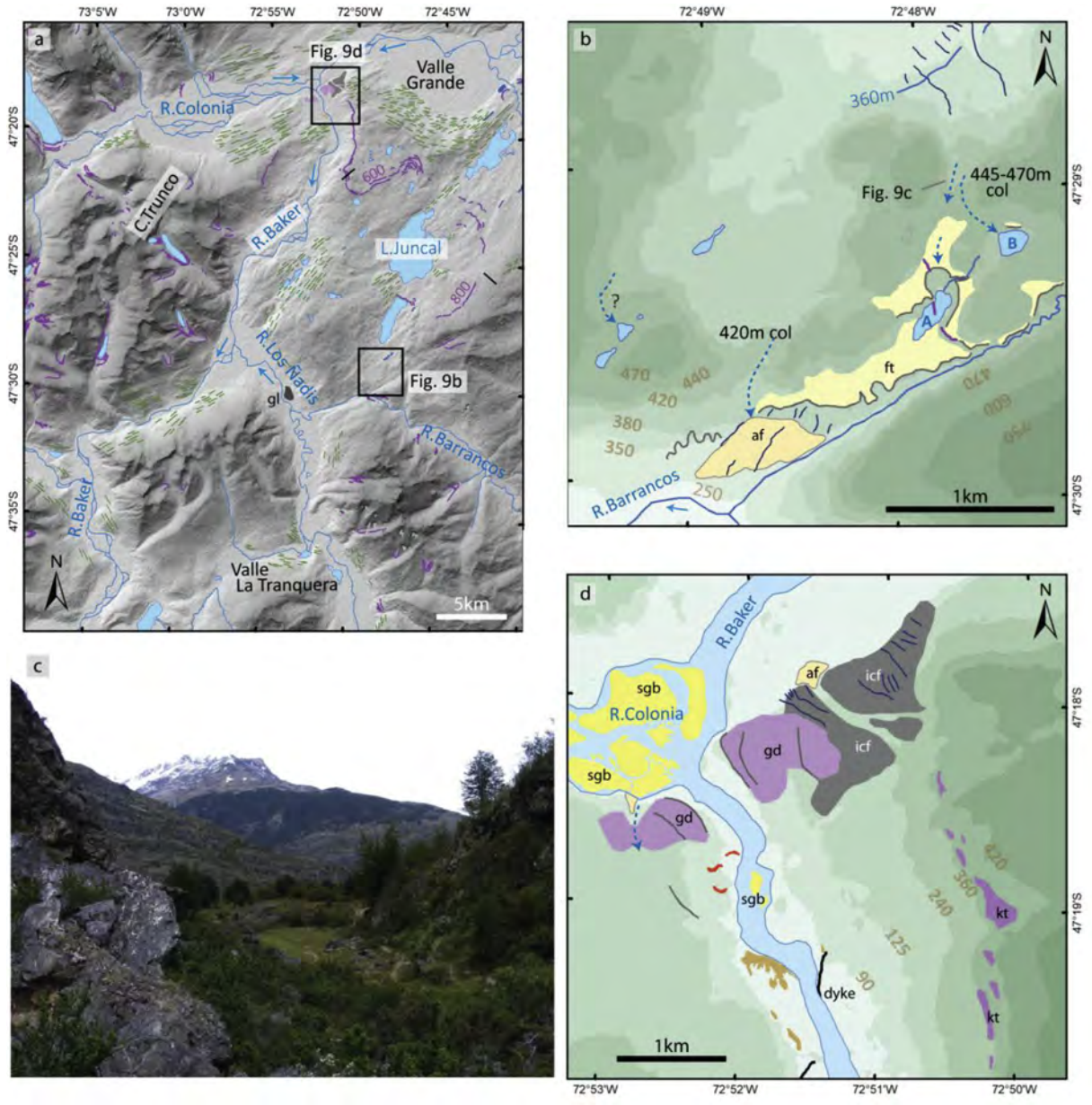

Fig. 9. (a) Geomorphological map of the Colonia-Barrancos sector. (b) Geomorphological map of the watershed zone between the Juncal and Barrancos valleys showing the evidence for water drainage over two col levels into the Barrancos Valley. We identify this locality as the missing drainage pathway of Hein et al. (2010) – see Fig. 2b. (c) Photo from the inner bedrock cut channel (~445–460 m asl) looking towards the Barrancos Valley. (d) Geomorphological map of the Colonia sector of the Baker Valley showing ice marginal landforms and evidence for high magnitude GLOF flows. Note the boulder bars are located upstream of a cross-valley dyke that controlled GLOF flow hydraulics through the reach. See Fig. 3c for legend.

Cochrane/Puerreydón (discussed in Section 4.1.1) though we note the latter event may have triggered the Lago Colonia GLOF by overtopping.

4.2. Palaeoshoreline analysis

Fig. 10a shows the results of the palaeoshoreline histogram analysis data alongside elevations of the major cols, spillways and ice dams from previous studies (Turner et al., 2005; Glasser et al., 2016), and our geomorphological mapping (Section 4.1). The data reveal major shoreline frequency peaks at 497 m asl, 394 m asl and 297 m asl for Lago Cochrane/Puerreydón, and 405 m asl and 299 m asl for Lago General Carrera/Buenos Aires (Fig. 10a). The peak frequency elevation for the upper lake in the Chacabuco valley is 588 m asl. Given the range of elevations on each of the isostatic shoreline curves (Fig. 10a) we have named the lake levels in relation to the controlling outflow rather than use elevations. We term the upper Chacabuco lake as the Rodolfo level. The upper lake level in the southern basin is termed the Caracoles level, the ~400 m asl lake in the northern basin we term the Deseado. The ~300 m asl lake level we term the Bayo following the recognition of a Bayo spillway (Glasser et al., 2016). We discuss later in the manuscript whether the unified Lago Chalenko forms at the Deseado or Bayo level.

In addition to the data for the main, previously mapped, shorelines (Turner et al., 2005; Hein et al., 2010; Glasser et al., 2016), the data reveal additional levels not previously associated with mapped outflows. We term these the sub-Caracoles level of Lago Cochrane/

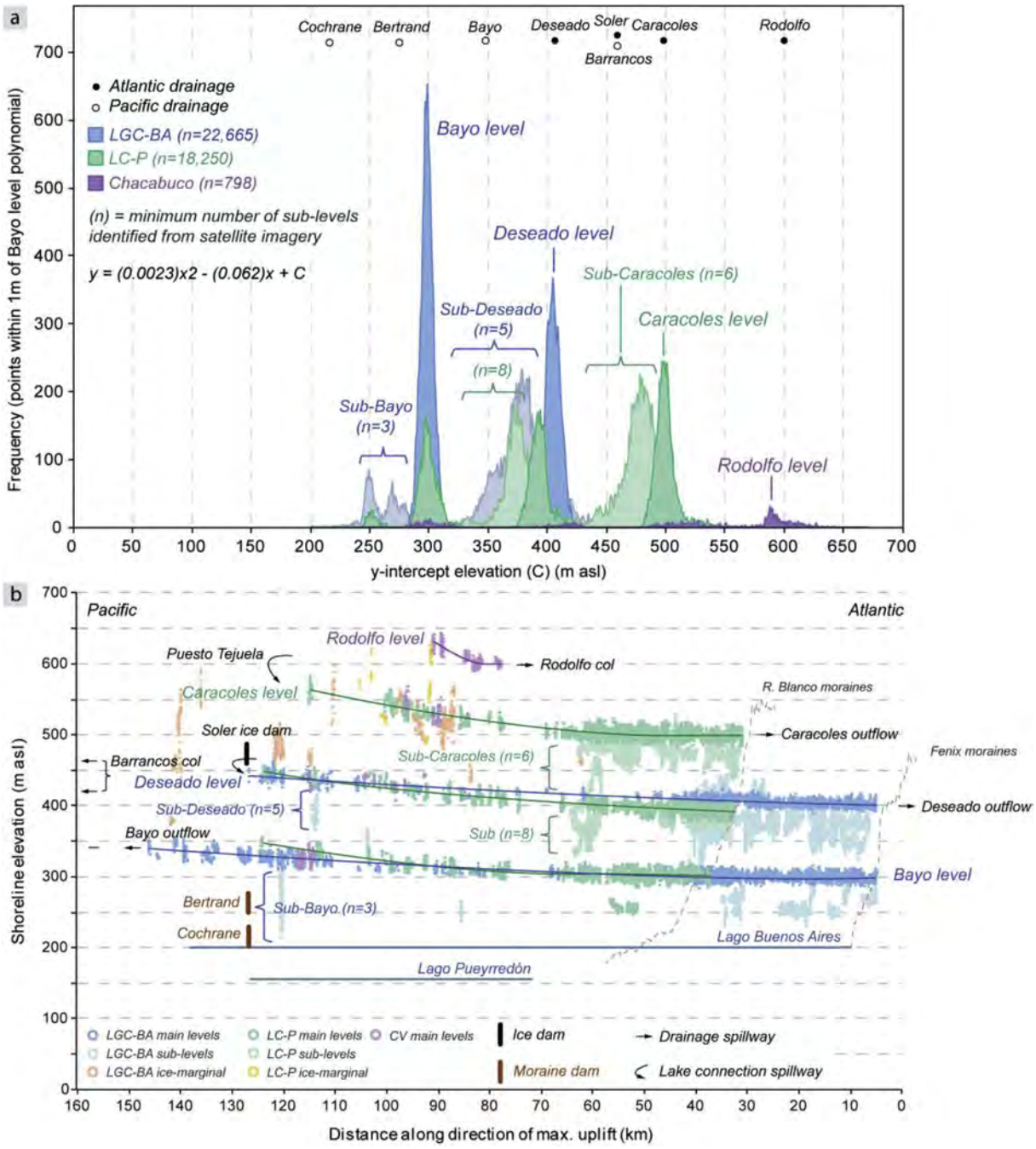

Fig. 10. (a) Shoreline histogram analysis showing multiple lake levels in the study area. A second order polynomial regression was fitted to Bayo level shoreline point data. The histogram peaks show the number of points that fit within 0.5 m of the polynomial regression line (equation shown on plot). Peaks indicate the number of points that fit the polynomial, with higher peaks indicating better constrained lake levels. Also shown are the elevations of key cols and inferred ice dam spillways. (b) Shoreline point elevations plotted against distance perpendicular to the maximum inferred uplift. Cols, inferred ice dam spillways and drainage pathways are annotated. For data see Bendle (2018).

Puerreydón (478 m asl), and the sub-Deseado (383 m asl) and sub-Bayo levels (249 m asl) in Lago General Carrera/Buenos Aires. These sub-levels comprise multiple, closely-spaced flights of shorelines, which cannot be differentiated due to the vertical resolution of the ASTER G-DEM. However given the recognition of the Barrancos spillway at ~460 m asl we refer to this lake level in the southern basin as the Sub-Caracoles level to contrast with the Deseado level of Lago General Carrera/Buenos Aires.

Fig. 10b plots the shoreline elevation data along the unidirectional (west-east) axis of maximum uplift, as defined through shoreline analysis, and coincides with former ice-lobe trajectories along the major outflow valleys. The lower lake levels reveal greater westwards extent of shoreline evidence, consistent with progressive ice-lobe recession and palaeolake expansion. The upper Rodolfo lake level extends for 13 km in Valle Chacabuco, compared to Lago General Carrera/Buenos Aires where the upper Deseado level extends for 122 km and the lower Bayo level for 141 km. As the relative age of palaeolake levels decreases, shoreline slope gradients also decrease in the southern basin. Here, the upper Caracoles level has the greatest degree of isostatic warping, with an average

gradient of 0.78 m km^{-1} towards the Patagonian Cordillera, compared to the Deseado and Bayo levels of 0.65 m km^{-1} and 0.51 m km^{-1} respectively. By contrast, the average gradients of the two main lake levels in the Lago General Carrera/Buenos Aires basin (northern basin) are similar, with 0.31 m km^{-1} for the Deseado compared to 0.30 m km^{-1} for the Bayo level. There are two potential interpretations of the data: (1) there is a smaller relative age difference between the Deseado and Bayo levels in the Lago General Carrera/Buenos Aires basin; and/or (2) rapid retreat of the Buenos Aires ice lobe followed by stabilisation in the western embayments of the basin, suggestive of limited change in ice extent between the latter stages of the Deseado level and the duration of the Bayo level. We note that this latter hypothesis is consistent with the ice-sheet simulation of Hubbard et al. (2005) who model a rapid retreat of the ice sheet from its eastern margins before stabilisation in the western embayment of Lago General Carrera.

A final observation reveals that average shoreline gradients are higher for the Lago Cochrane/Puerreydón levels compared to the same levels for Lago General Carrera/Buenos Aires e.g. the Bayo level shoreline gradient is 0.51 m km^{-1} for the former, compared to 0.30 m km^{-1} for the latter. This may reflect ice-sheet thinning along the ice divide between the Northern Patagonia Icefield and Monte San Lorenzo (Fig. 1) modelled by Hubbard et al. (2005), creating an additional axis (north-south) of isostatic uplift that we cannot differentiate using our methodology. For the ~13.5 ka time-slice, the Hubbard et al. (2005) ice-sheet model suggests that outlet glaciers of the Northern Patagonian Icefield and Monte San Lorenzo had separated, and the Baker valley was ice-free, when ice remained in the western embayments of Lago General Carrera. This implies a greater loss of ice thickness in the southern basin, with >1500 vertical metres of ice loss here compared to 1000 m in the western embayment of Lago General Carrera, which could explain the contrasting shoreline gradients.

4.3. Altitudinal-based review of geochronology

Recalibrated ages (Table SM.1) relevant to the chronology of palaeolake evolution are plotted against sample altitude in Fig. 11. The precision of ages differs according to technique, with CND boulder ages and OSL shoreline dates exhibiting greater uncertainties than radiocarbon dates from basal organics.

4.3.1. The northern basin (Lago General Carrera/Buenos Aires)

The onset of ice-lobe retreat from the Fenix moraines (dates not in Fig. 11) in eastern Lago Buenos Aires is precisely constrained by the FCMC17 varve record (Bendle et al., 2017b), which is time-anchored by the Ho tephra from Cerro Hudson (Weller et al., 2014). Bayesian age modelling constrains the timing of retreat from the late-LGM Fenix and Menucos moraines to 18.1 ± 0.21 and 17.7 ± 0.12 cal ka BP, respectively. The varve chronology and sedimentology implies that the Buenos Aires ice-lobe maintained a position in the eastern lake basin until 16.9 ± 0.12 cal ka BP (Bendle et al., 2017b). The next dated ice positions in the basin are those from the Bertrand moraine complex (Fig. 3, this study) that date an ice margin at the contemporary Lago General Carrera outflow from 15.8 ± 1.1 to 13.7 ± 0.8 ka. These ages are older than the previously dated CND samples from the Lago Negro moraine (~250 m asl), which span 10.2–11.4 ka (Table SM1). This ice margin was also dated by Bourgois et al. (2016), who presented a CND age of 17.6 ± 3.8 ka. Glasser et al. (2016) used OSL to date lake shorelines with ages for the 460–520 m asl lake level spanning 13.5-10.5 ka, whilst dates range between ~15.5-7.0 ka for the ~400 m asl lake level and ~12.0-7.0 ka for the ~300 m asl level.

4.3.2. The southern basin (Lago Cochrane/Puerreydón and Chacabuco valleys)

The Columna and Río Blanco moraines of the Chacabuco and Puerreydón ice-lobes respectively overlap with ages spanning 19–25 ka (Fig. 11). There is no data on intermediary ice positions in the Cochrane/Puerreydón basin. A single erratic was dated to 17.3 ± 1.1 ka but this was interpreted by Hein et al. (2010) as having been shielded by lake water and dates lake level fall rather than ice retreat. The timing of ice retreat in the Chacabuco valley is indicated by the CND samples (463–586 m asl) from the Maria Elena moraines (*72°21'08"W 47°03'59"S*, Fig. 6a), which have a recalculated weighted mean age of 16.2 ± 0.6 ka (Boex et al., 2013). Three radiocarbon dates from Lago Augusta (440 m asl, Fig. 6a), which is located on the ice proximal side of the Maria Elena moraines, provide a minimum age of 15.6–14.8 cal ka BP for the end of glaciolacustrine sedimentation (Villa-Martínez et al., 2012) and the ice margin here must have pre-dated the lake sediments. The earliest age of ~19 cal ka BP for lake sedimentation was excluded from the Lago Augusta age model by Villa-Martínez et al. (2012), however we note the similar Lago Edita ages from this higher altitude lake (Henríquez et al., 2017). Further ice retreat in the Chacabuco valley is demonstrated by CND ages for three boulders from moraine mounds near the Baker-Chacabuco confluence (Glasser et al., 2012): 11.2 ± 0.7 ka (309 m); 11.5 ± 0.7 ka (314 m); and 14.6 ± 0.8 ka (350 m asl).

The 350 m asl Chacubuco CND sample is at a similar elevation to the radiocarbon ages from peat and macrofossils at kettle holes at the Salto moraines (*72°39'19"W 47°17'52"S*, Fig. 6c), which span ages of 13.4–16.5 cal ka BP (Turner et al., 2005). A landform interpreted by Turner et al. (2005) as a kame delta at 340 m asl in the Nef Valley, but mapped as a raised delta in Fig. 6a (*72°58'10"W 47°08'00"S*), was radiocarbon dated to 13.0–12.7 cal ka BP. Basal radiocarbon dates were also obtained from kettle holes in the Cochrane and Maiten valleys (<200 m asl) that date to 13.0-12.7 and 12.8–12.2 cal ka BP respectively. The youngest age from our database is the OSL sample (CL1256, 7.8 ± 0.5 ka) from the loess deposit capping slackwater flood deposits (this study) located at ~210 m asl in the Nef-Chacabuco reach of the Baker Valley.

5. Discussion

In this section we firstly synthesise the palaeoshoreline (Section 4.2) and geochronology datasets (from Sections 4.2 and 4.3, respectively) so that we can evaluate previously published palaeolake evolution models (Section 5.2). These evaluation sections inform the Bayesian age model presented in Section 5.3, which underpins a new model of palaeolake evolution (Section 5.4) that is used in a regional evaluation of continental scale drainage reversals in southernmost South America (Section 5.5).

5.1. Evaluating regional geochronology with palaeoshoreline data

In this section we bring together the main implications for palaeolake evolution of the new geomorphological and geochronological datasets. In Fig. 12 we present the altitudes of the key sampled locations for geochronology on the shoreline isostasy curves. An important finding is that many of the morainic boulders sampled for CND ages to date ice margins were likely shielded beneath lake water. Comparing the Chacabuco moraine samples from Glasser et al. (2012) with the Caracoles and Bayo levels, Fig. 12 demonstrates that all three of the boulders sampled by Glasser et al. (2012) were submerged beneath the Caracoles level, with two sampled beneath the Bayo level. This data explains the observed differences in CND ages as the 14.6 ± 0.8 ka sample was located between the Caracoles and Bayo levels, compared to the ages of

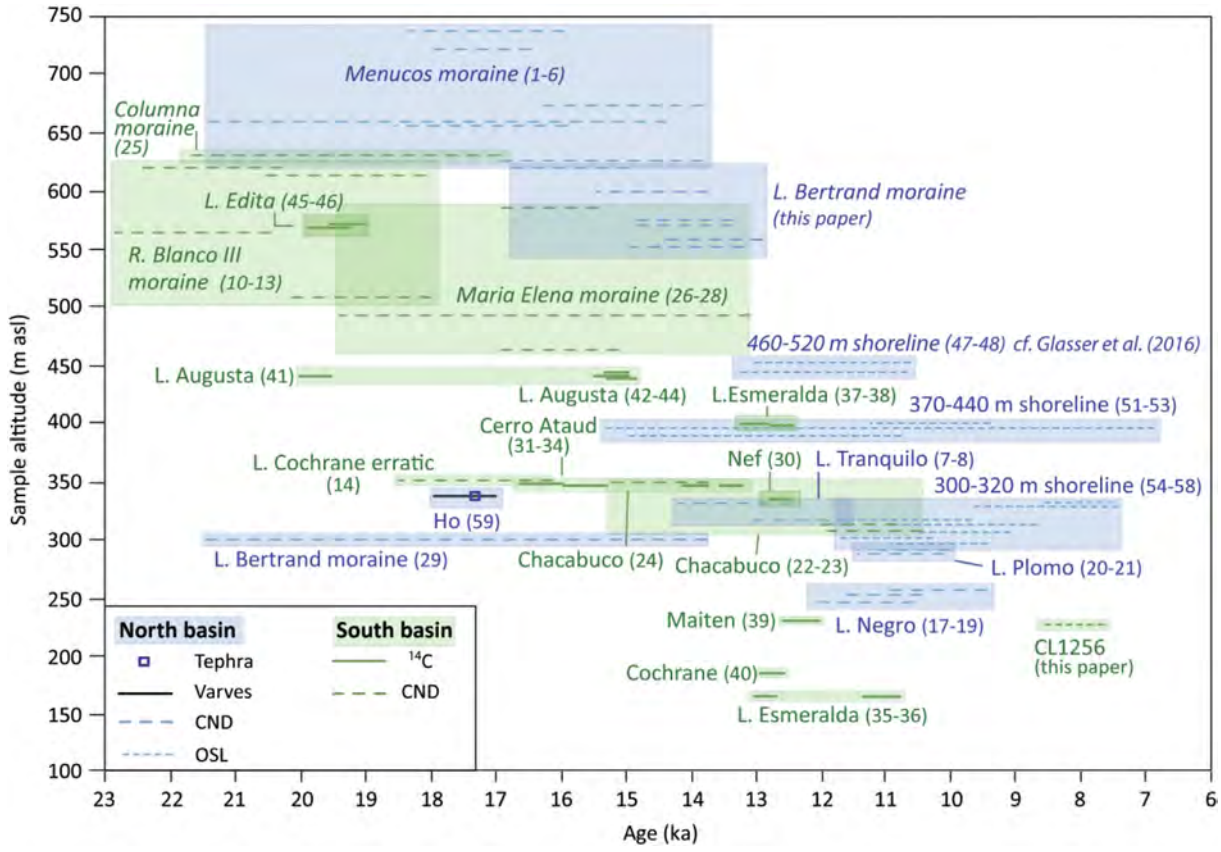

Fig. 11. Age versus sample altitude for the compiled geochronology database (see Supplementary Materials Table SM1). Numbers in brackets indicate sample numbers listed in Table SM1, and boxes are drawn around multiple samples from the same landform. The CND and OSL ages from this study are presented in Table 1. Samples are plotted according to dating method and whether they are from the northern or southern basins (see Fig. 1b). The length of the symbols are the calculated errors (Table 1 and SM1). Note the position of the dated Ho tephra, which anchors a varve chronology from Lago General Carrera/Buenos Aires (Bendle et al., 2017b) improving age precision for the onset of deglaciation.

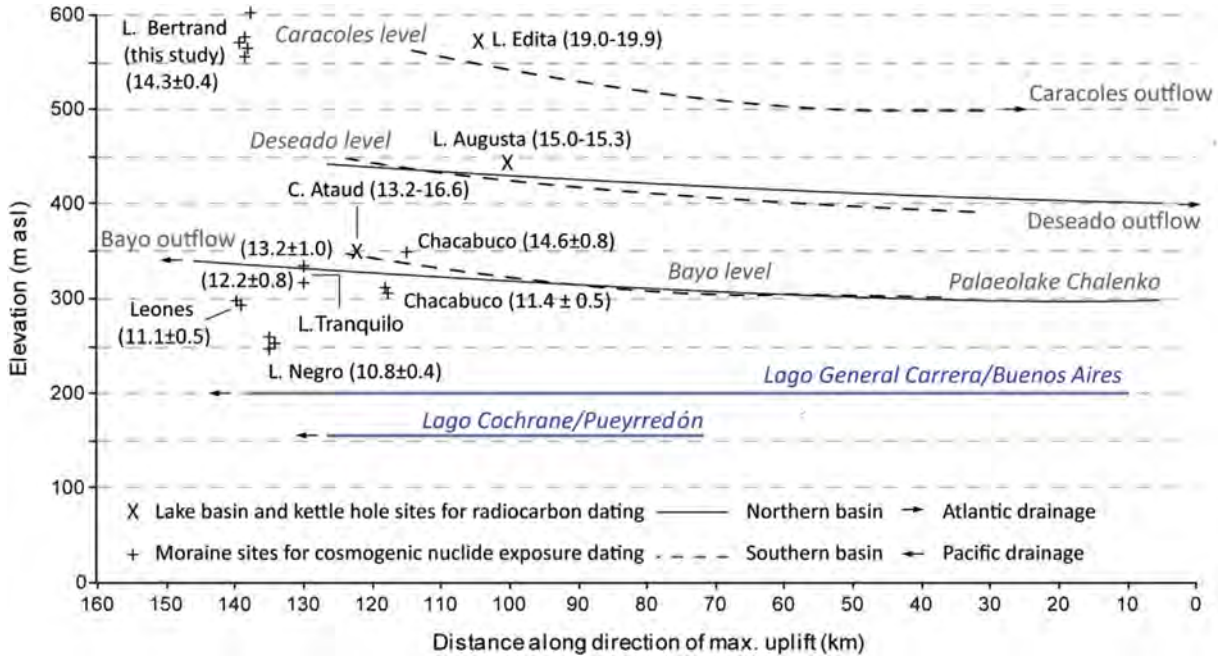

Fig. 12. Selected geochronology sample elevations plotted against the isostatic shorelines presented in Fig. 10. Weighted mean ages and errors for CND ages, the modelled ages for Lago Augusta (SM.2.1) and the calibrated age ranges for the other radiocarbon dated sites are shown in brackets. Note that CND ages from various moraine sites are located beneath the Bayo lake level. The two lower elevation Chacabuco boulders (11.3 ka) are younger than the higher elevation boulder (14.6 ka) that was exposed above the Bayo lake level. The Lago Bertrand weighted mean (this study) is calculated by using the five dates selected for the Bayesian age model (see SM 2.2).

11.2 ± 0.7 ka and 11.5 ± 0.7 ka date boulders from beneath the Bayo level. Lake water shielding (Schaller et al., 2002; Fabel et al., 2010; Balco, 2014) therefore provides an alternative interpretation for the older age, previously considered an outlier by Glasser et al. (2012). The lower altitude boulders were likely exposed by the Bayo lake level fall and therefore date drainage of Lago Chalenko rather than a glacier readvance coinciding with the Northern Hemisphere Younger Dryas. This interpretation is further supported by our new CND ages (14.3 ± 0.4 ka), which predate the Lago Negro moraines which were submerged beneath Lago Chalenko (Fig. 3).

The sedimentology of the Lago Negro moraine (Fig. 5) demonstrates an ice-lake margin with the glacier discharging into a higher lake stand than the present lake, consistent with the local shoreline evidence for higher lake stands (Fig. 3a). As demonstrated on Fig. 12, the Lago Negro moraine ages were also located beneath the Bayo lake level and overlap, within dating errors, the two lower altitude boulders of the Chacabuco moraine. The weighted mean age of the five youngest dates from the Lago Bertrand moraine (Table 1), all sampled from moraines located above 500 m asl (Fig. 12), is 14.3 ± 0.4 ka compared to 10.8 ± 0.4 ka for the Lago Negro moraine boulders (Glasser et al., 2012). Given the sedimentological evidence for subaqueous moraine formation, the spatial extent of the mapped 340 m shoreline, and the >3000 year discrepancy between the CND ages, we infer the Negro boulders were likely exposed by the Bayo lake level fall. The ages from the Leones and Tranquilo erratics (Glasser et al., 2012) are also consistent with this interpretation (Fig. 12).

The timing of palaeolake level falls can also be evaluated using the radiocarbon dating of basal organics from enclosed lake basins and kettle holes (Turner et al., 2005; Villa-Martínez et al., 2012). At Lago Augusta in the Chacabuco valley the radiocarbon dating of the transition from glaciolacustrine to gyttja sedimentation provides critical age control for lake level drop below the local 460 m asl shoreline mapped in the Nef-Chacabuco sector (Fig. 6). Lago Augusta became a small enclosed basin, with a watershed at 450 m asl (Villa-Martínez et al., 2012), following this lake level fall prior to the modelled age of 15.3–15.0 cal ka BP (SM 2.2). The altitude of Lago Augusta is beneath the Caracoles shoreline curve (Fig. 8) so these radiocarbon dates must post-date abandonment of the Caracoles outflow and the Río Pinturas drainage route to the Atlantic from the southern basin.

Turner et al. (2005) also aimed to constrain lake level falls using basal radiocarbon ages by targeting kettle hole basins at altitudes between and below their upper and lower unified lake levels. One anomalous finding was the early ages of 16.0–13.0 cal ka BP from the Cerro Ataud kettle holes (Fig. 6c), which were chosen to date drainage of the Bayo level lake. To explain the early ages, Turner et al. (2005) hypothesised that isostatic adjustment may have raised the kettle holes above the local lake level, with the base of the mapped palaeoshoreline scarp lying beneath kettle hole altitude. Turner et al. (2005) hypothesised that the samples were therefore contemporaneous to, rather than post-dating, the Bayo lake level. Our shoreline isostasy data and geomorphological mapping lends support to this hypothesis, though higher resolution DEMs with greater vertical precision are needed to test this further, and caution is still needed with regards the oldest ages that appear to pre-date abandonment of the Caracoles lake level.

With regards the OSL ages from palaeoshoreline deltas and beaches, the highest altitude samples at 460–530 m asl (Fig. 11) were taken from sites located above our highest reconstructed lake levels in the northern basin (Fig. 10). For the Deseado level OSL samples there is a wide range of ages, including errors that span 15.5-7.0 ka, overlapping the dates from the Bayo level (12.0-7.5 ka). The Bayo level OSL dates in turn overlap the mean age of 11.2 ka for the six Bayo lake level CND ages shielded by lake waters (Fig. 12), and post-date basal radiocarbon ages for Bayo drainage (12.8 cal ka BP, Turner et al., 2005). These OSL ages are therefore difficult to place in the context of the geomorphological evidence presented in this paper.

5.2. Evaluating published models of palaeolake evolution

In this section, we compare our new data, and interpretation of published geochronology (summarised in Table 2), with previously

Table 2
Summary of the evidence presented in this paper for reinterpretation of the Late Quaternary palaeohydrology of central Patagonia (46–48 °S).

Previous interpretation	Reference	New interpretation/hypothesis and supporting evidence
400 m united lake forms between at 16.5-15.0 ka (Fig. 2a)	Turner et al. (2005); Hein et al. (2010)	New CND ages from Bertrand moraine (Fig. 3) show Soler ice (~160 km^2) blocking the upper Baker valley from ~15.9-13.7 ka. An alternative hypothesis is that glaciers retreated sufficiently to allow Pacific drainage prior to the Antarctic Cold Reversal readvance as suggested in northern (Moreno et al., 2015) and southern (Hall et al., 2013) Patagonia by rapid ice retreat to the Andean Cordillera. However, there is no landform or sedimentological evidence demonstrating that at present, and we note the larger ice sheet size in central Patagonia.
300 m Lago Chalenko forms between 16.5-15.0 ka (Fig. 2b)	Turner et al. (2005); Hein et al. (2010)	New CND ages from Bertrand moraine (Fig. 3) show Soler ice (~160 km^2) blocking the upper Baker valley from ~15.9-13.7 ka. More dating evidence is required to determine the timing of Lago Chalenko formation but the Bayesian age model (Fig. 13) suggests likely formation towards the end of the Antarctic Cold Reversal.
First Pacific drainage reversal at 12.8 ka	Mercer (1976); Turner et al. (2005)	Shoreline data confirms lake level drop at Lago Augusta relates to abandoned Caracoles drainage (Fig. 12). Atlantic drainage was, therefore, likely abandoned in the Southern Basin by 15.3–15.0 cal ka BP (Lago Augusta, Villa-Martínez et al., 2012; Fig. S2) by possible catastrophic drainage at the Barrancos col (Fig. 9).
Endorheic lake (12.9-10.9 ka) at 300 m asl (Fig. 2c)	Bourgois et al. (2016)	We identify new drainage pathways via the Barrancos col or a Soler glacier ice dam so endorheic drainage need not be invoked. No palaeoecological evidence for sufficient drying of climate. Sedimentology of raised deltas (e.g. Bell, 2008) suggests perennial river flow.
Maximum post LGM ice extent coinciding with the Northern Hemisphere Younger Dryas	Glasser et al. (2012)	Bertrand moraine (Fig. 3) dated to the Antarctic Cold Reversal, and shoreline analysis (Fig. 12) indicates likely lake water shielding of boulders used to infer a Younger Dryas age.
Glacier readvance at 10.9-7.9 ka creating a 520 m asl lake in the Northern Basin (Fig. 2d)	Bourgois et al. (2016)	There is no evidence for such a significant readvance at this time and morpho-stratigraphic data from Fenix Chico (Bendle et al., 2017b) indicates the maximum lake level of Lago General Carrera/Buenos Aires was at the Deseado level (~400–440 m asl, Fig. 10).
Bayo drainage pathway opens at 10.5 ka (Fig. 2e)	Glasser et al. (2016)	Shoreline data (Fig. 10) supports a Bayo drainage hypothesis but Lago Chalenko likely formed at the end of the Antarctic Cold Reversal (Fig. 13). It is possible that the Northern Basin drained via the Bayo col prior to formation of Lago Chalenko but more data is needed to test this hypothesis.
315-260 m asl unified lake at 8.0 ka draining to Lago O'Higgins (Fig. 2f)	Glasser et al. (2016)	Geomorphic evidence from the Baker valley shows multiple GLOF events flowed down the subaerial valley by 8.0 ka, likely from moraine dammed lakes formed following Lago Chalenko drainage.

published lake models (Fig. 2). There is limited geomorphological evidence (this paper, Bendle et al., 2017a and 2017b) for proposed high (>500 m asl) elevation lake levels of LGC–BA - the Glasser et al. (2016) upper precursor lake (not illustrated in Fig. 2) and the Holocene transgression (Fig. 2e) of Bourgois et al. (2016). The geomorphology, sedimentology and stratigraphy of the Fenix Chico valley at the eastern end of Lago Buenos Aires (Bendle et al., 2017b) demonstrates the lake formed at the Deseado level at ~18.1 ka with no evidence for a later lake transgression above this level. Our data, including the palaeoshoreline analysis (Fig. 11), support the view of Martinod et al. (2016) that the upper level raised deltas and shorelines relate to ice marginal lakes dammed by the lateral margins of the Buenos Aires ice lobe.

The new CND ages (Fig. 3b) from the Bertrand moraines demonstrate that ~160 km^2 of Soler Glacier ice blocked the Baker valley ~14.3 ± 0.4 ka. These dates and the mapping of a new spillway at the Juncal-Barrancos watershed (Fig. 9b and c), demonstrate that formation of Lago Chalenko at the upper ~400 m asl (Deseado) level (Fig. 2a) need not be inferred to explain lake drainage pathways. Drainage via the Barrancos col and spillway (locally 420–470 m asl) occurred by 15.3–15.0 cal ka BP (Lago Augusta), which supports the Hein et al. (2010) timing for abandonment of the Caracoles spillway by 15.5 ka. Hein et al. (2010) left open the possibility of a Baker valley drainage pathway to the Pacific at 15.5 ka (Fig. 2b) - the Barrancos spillway provides the first geomorphological evidence for this route. This indicates a first Atlantic-Pacific drainage event by 15.3–15.0 cal ka BP, rather than 12.8 cal ka BP (Mercer, 1976; Turner et al., 2005) or 10.5 ka (Glasser et al., 2016), though we acknowledge the lack of geomorphological evidence for the drainage pathway to the Pacific (inaccessibility and forest cover have, to date, prevented detailed geomorphological mapping in this sector).

We provide the first field geomorphological evidence for an ice margin blocking the lower Baker valley, based on the landform assemblage at the Baker-Colonia confluence (Fig. 9d). Ice marginal landforms located at altitudes between the Bayo and sub-Caracoles lake levels suggest this ice margin was associated with damming of the Bayo lake level so drainage of the southern basin would likely have been through the Baker valley to Lago General Carrera/Buenos Aires, as inferred in the unified lake models of Turner et al. (2005), Hein et al. (2010) and Glasser et al. (2016).

Finally, our geomorphological evidence does not support a unified 315-260 m asl lake level extending in to the lower Baker valley and dammed by a still coalesced Patagonian Ice-sheet in the Pacific fjords (Glasser et al., 2016). The palaeolake evidence at the Salto moraines suggests punctuated drainage occurred down to the 150 m asl level where lake level stabilised, likely dammed by the moraine at the Baker-Colonia confluence (Fig. 9d). Flood geomorphology (Fig. 8) reveals GLOF drainage of Lago Colonia as well as further high magnitude floods through the subaerial Baker and Cochrane valleys from separate lakes in the northern and southern basins, suggesting at least three moraine dammed lakes in the Baker catchment following drainage of Lago Chalenko.

In summary, through new geomorphological and geochronological datasets, we have been able to establish morphostratigraphic relationships between glacial, lacustrine and glaciofluvial landforms in key sectors of the Baker valley. Through this approach, we have been able to identify a new spillway at the Juncal-Barrancos watershed, and have hypothesised that ice dams blocking the upper and lower Baker valley may have existed at the same time. This is important because previous interpretations have been based on the altitudes of available bedrock cols, however the new dating for Soler ice blocking the upper Baker valley when lake level falls were happening in the southern basin (e.g. Villa-Martínez et al., 2012) means that drainage from the southern to northern basin could have happened at the Soler ice margin. In the next section we present a Bayesian age model based on our new data sets and geomorphological interpretation.

5.3. Bayesian age model of palaeolake evolution

The evaluation in Sections 5.1 and 5.2 was used to develop a Bayesian age Sequence model (Fig. 13) for palaeolake evolution (see Supplementary Materials, SM2.2), including modelling age constraints for the formation of Lago Chalenko and its subsequent drainage. To model these events, the key ages prior to lake unification were provided by the Lago Bertrand moraine samples (Table 1), which date glacier extent for ~160 km^2 of Soler ice blocking the upper Baker valley (Fig. 3). Because the formation of Lago Chalenko must post-date retreat from the Bertrand moraines, in the model this event is constrained by the Bertrand moraine dates and four ages we interpret as dating the Bayo lake level. Drainage of Lago Chalenko at the Bayo lake level occurred prior to the basal radiocarbon dates from Cochrane and Maiten kettle holes (Turner et al., 2005), and the CND ages from Glasser et al. (2012) where the boulders are demonstrated in Fig. 12 to have been exposed by lake drainage.

We define Phase 1 of the age model (Fig. 13) by the current end date for varve sedimentation in the fixed varve chronology of FCMC17 (16.94 ± 0.12 cal ka BP), where the varve sedimentology and thickness record suggests a rapidly retreating, calving ice margin (Bendle et al., 2017b). The precise position of the ice margin at this time is unknown but was interpreted as being situated in the eastern basin of Lago Buenos Aires (Bendle et al., 2017b), likely >120 km east of the Lago Bertrand moraine complex (Fig. 1). The start of Phase 2, Lago Bertrand moraine formation, was modelled to 15.0–14.2 cal ka BP (95.4%) suggesting ~3.0 ka for >120 km of ice retreat of the Buenos Aires ice-lobe. The CND and modelled ages constrain an Antarctic Cold Reversal age for the Bertrand moraine, although we interpret a possible earlier stabilisation once ice retreated to the bedrock pinning point at the contemporary Lago General Carrera outflow (Barr and Lovell, 2014). A similar chronology was obtained for Glacier Tranquilo (Monte San Lorenzo), where an extensive moraine dating to the ACR was preceded by recessional moraines (Sagredo et al., 2018). As previously stated the Bertrand moraines lie ~5° south of the geographic range of influence of the ACR inferred from palaeoclimate modelling (cf. Pedro et al., 2016) so provide empirical evidence in support of an ACR glacier re-advance. Ice- sheet modelling of the Northern Patagonian Ice-sheet, driven by the Antarctic Vostok ice core record, suggests a slight ice sheet volume increase during the Antarctic Cold Reversal (Hubbard et al., 2005), and we note the modelled Soler ice limit broadly matches our empirical evidence from the Bertrand moraines.

The modelled ages for the Bertrand moraines overlap the P-Sequence age modelled dates of 15.3–15.0 cal ka BP (SM2.2) for the isolation of the closed Lago Augusta basin, a minimum age for abandonment of Lago Cochrane/Puerreydón drainage over the Caracoles col and opening of the Barrancos spillway. Lake unification, and the formation of Lago Chalenko, is modelled to start at 14.2–13.7 cal ka BP. Assuming the retreat of ice from the Bertrand moraines occurred at the end of the Antarctic Cold Reversal then the formation of Lago Chalenko would have likely happend by ~13.0 ka. The start of the Lago Chalenko drainage phase was modelled to 12.4–11.8 cal ka BP, post-dating Turner et al.'s (2005) 12.8 cal ka BP interpretation. Finally, the GLOF phase was modelled to 9.8–8.0 cal ka BP. The Bayesian age model is used to underpin a new palaeolake evolution model presented in Section 5.4.

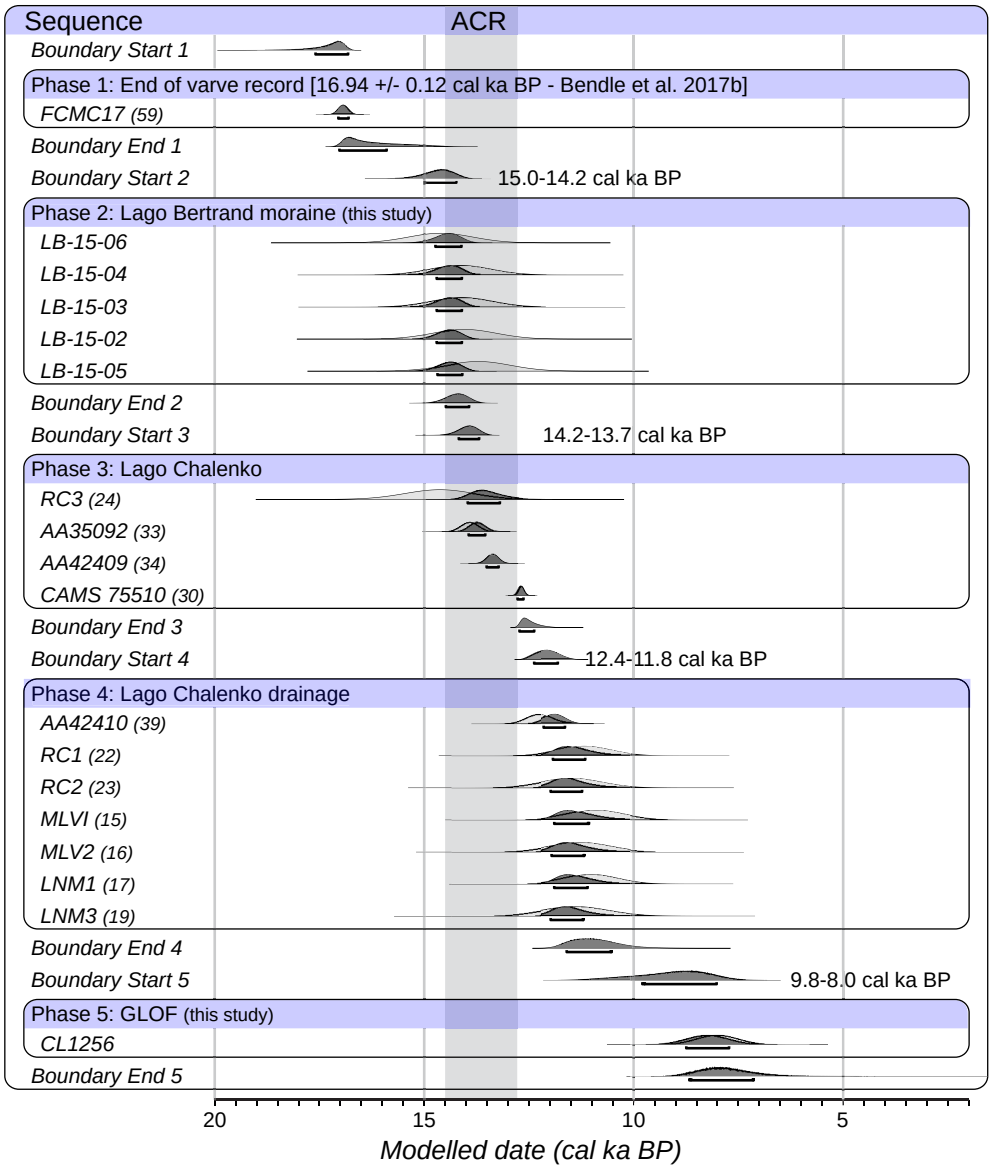

Fig. 13. Bayesian age Sequence model for key palaeolake evolution events through the main Baker valley. Phase (1): end of varve sedimentation at Fenix Chico. Phase (2): formation of the Bertrand moraine complex (this study). Phase (3) Formation of Lago Chalenko following retreat of the Soler Glacier from the Bertrand moraines and the opening of the Baker valley. Phase (4) Lago Chalenko drainage. Phase (5) GLOF events. The timing of the Antarctic Cold Reversal is shown. Numbers in parentheses refer to sample numbers in Table SM 1.

5.4. Event sequence of palaeolake evolution at 46–48 °S

The timings of the key phases of the Bayesian age model are presented in Fig. 14 alongside the Western Antarctic Ice-sheet Divide Core (WDC) palaeotemperature record (WAIS Members, 2013) and our inferred event sequence of lake drainage events and glacier dynamics. We use the age modelling and our geomorphological datasets to reconstruct an 8 stage event sequence of palaeolake evolution, presented in Fig. 15 and summarised in Table 3.

Stage 1 18.0-17.0 ka (Fig. 15a)*:* The onset of deglaciation results in ice retreat from the eastern moraine systems and the formation of proglacial lakes in the Buenos Aires, Chacabuco and Puerreydón valleys at the Deseado, Rodolfo and Caracoles levels respectively (Turner et al., 2005; Glasser et al., 2016). The onset of lake formation in the Buenos Aires basin is dated by the onset of the FCMC17, tephra constrained, varve record at 18.1 ± 0.21 cal ka BP. Ice position was still likely in the eastern Buenos Aires basin at the end of the varve sequence at 16.94 ± 0.12 cal ka BP (Bendle et al., 2017b).

Stage 2 17.0-16.0 ka (Fig. 15b)*:* In the southern basin, the retreat of Chacabuco ice to the Maria Elena moraine (Fig. 6a), dated to a recalculated weighted mean age of 16.2 ± 0.6 ka (Boex et al., 2013), leads to abandonment of the Rodolfo col, with drainage from the Chacabuco valley to Lago Cochrane/Puerreydón over the Puesto Tejuela spillway (*72°25'45"W 47°08'42"S*, Fig. 6a), as proposed by Glasser et al. (2016). This is associated with the Caracoles level of the southern basin, with outflow drainage to the Atlantic via Río Pinturas. Ice likely retreated further westwards to the Chacabuco moraines, leading to the onset of glaciolacustrine sedimentation at Lago Augusta. In the northern basin ice retreated towards the Lago Bertrand moraines at the western end of Lago General Carrera. The ice-lake margins would differ at these two ice margins with deep lake waters (>300 m) at the Baker-Chacabuco confluence, while the Buenos Aires ice-lobe would have started retreating into shallower waters (<250 m) compared to the deepest part of the lake basin.

Stage 3 16.0-15.3 ka (Fig. 15c)*:* The Nef and Colonia glaciers

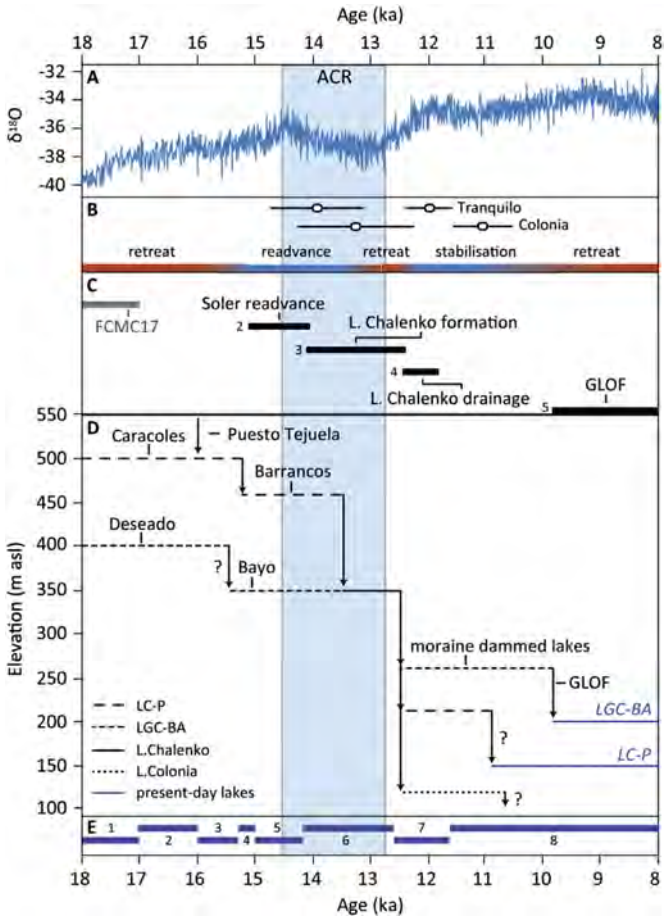

Fig. 14. Summary of palaeolake evolution during the Last Glacial-Interglacial Transition. a) WDC $\delta^{18}O$ (palaeotemperature) record demonstrating the Antarctic Cold Reversal (WAIS Members, 2013); b) Inferred glacier dynamics with CND ages from selected moraines of the Tranquilo (Sagredo et al., 2018) and Colonia (Nimick et al., 2016) glaciers shown; c) Bayesian age model phases (2–5) from Fig. 13 (this paper) and the FCMC-17 varve record duration from the onset of deglaciation (Bendle et al., 2017b); d) inferred lake levels and drainage events; and e) Stages of the palaeolake evolution model presented in Section 5.4 (this paper).

separate and retreat westwards from the Baker-Chacabuco confluence (Fig. 6a), creating two ice dams, one upstream and one downstream of the Baker-Chacabuco confluence. Colonia Glacier maintains an ice dam blocking the downstream Baker valley, with ice surface gradient dipping eastwards from the Andean Cordillera towards the lake margin. In Valle Grande lake waters would have been ~400 m deep. The retreat of the Nef Glacier allows lake water to reach the Soler Glacier. Here the eastwards ice surface gradient slopes towards the General Carrera basin, therefore, because water flows perpendicular to contours of equal hydraulic potential at the glacier bed, the southern basin could have drained either subglacially, englacially or around the margins of Soler Glacier into the northern basin. This phase coincides with the abandonment of the Caracoles outflow and the Río Pinturas drainage pathway.

Stage 4 15.3-15.0 ka (Fig. 15d): The start of this phase is triggered by collapse of an ice dam at the Barrancos spillway (445–470 m asl) enabled by unzipping of the Northern Patagonian Icefield and Monte San Lorenzo ice sources in the Juncal valley (Fig. 9). This led to an Atlantic-Pacific drainage reversal from the southern basin releasing ~37 km^3 of meltwater (Table 3). The event is dated by the isolation of the Lago Augusta basin at ~450 m asl (Villa-Martínez et al., 2012), with a modelled age of 15.3–15.0 cal ka BP (Fig. 13). Ice position in the northern basin stabilised in the western embayment likely due to its retreat to a bedrock pinning point, with the ice no longer calving into the deep open waters of the lake basin.

Stage 5 15.0-14.2 ka (Fig. 15e)*:* This stage coincides with the onset of the Antarctic Cold Reversal (14.5-12.8 ka) and features readvance of the Soler Glacier ice margin at the Lago Bertrand moraines (15.0–14.2 cal ka BP). Although the ice position at Lago Bertrand is clearly defined for this stage the meltwater pathway from the southern sector is not. Water may have exited over the Barrancos col at 420 m asl, so maintaining a Pacific pathway, or was routed to Lago General Carrera through the Bertrand valley via englacial or supraglacial drainage of the Soler Glacier, which would imply a lower (Bayo) lake level in the northern basin, so it is possible the Bayo drainage pathway had opened by this stage. The opening of the Bayo drainage pathway was dated to ~10.5 ka in the Glasser et al. (2016) palaeolake model, based on a single OSL date to the west of the col (Glasser et al., 2006). However, two CND-dated erratics, 13.2 ± 1.0 ka (336 m asl) and 12.2 ± 0.8 ka (317 m asl) (Table SM1), on ice scoured bedrock to the east of the Bayo col (Glasser et al., 2006), in our model are reinterpreted as dating lake drainage rather than ice retreat. We note the altitude of the older of the two sampled boulders is close to the inferred Bayo glacioisostatic shoreline curve (L. Tranquilo boulders, Fig. 12) so shielding by the Bayo level may have been minimal, hence the different ages. We interpret these dates as providing an earlier minimum age for the opening of the Bayo drainage pathway.

Stage 6 14.2-12.6 ka (Fig. 15f)*:* At the end of the Antarctic Cold Reversal the Soler Glacier retreats opening the upper Baker valley to allow unification of the northern and southern basins forming Lago Chalenko (modelled age 14.2–13.7 cal ka BP). Whether this happened when the lake was at the Deseado or Bayo levels is equivocal at present with regards morpho-stratigraphic evidence and lack of a high resolution DEM to distinguish lake shoreline altitudes. We note, however, in addition to the possibility of Bayo drainage during Stage 5, the dating evidence from the southern basin, such as the Salto kettle holes (Turner et al., 2005), and the 350 m Chacabuco CND sample, overlap the Antarctic Cold Reversal age for the Bertrand moraines suggesting Lago Chalenko may have formed at the Bayo level. Under this scenario 182 km^3 of water would have been released to the Pacific from LGC–BA, rather than 509 km^3 if Lago Chalenko were fully formed at the Deseado level prior to lake level fall (Table 2).

Stage 7 12.6-11.7 ka (Fig. 15g)*:* The lower Baker valley drainage pathway opens following continued ice retreat allowing drainage of Lago Chalenko and abandonment of the Bayo outflow. As lake level fell, large valley floor moraines were exposed. These prevented full drainage of Lago Chalenko but instead impounded moraine-dammed lakes. We identify three such lakes that include Lago Colonia in Valle Grande, Lago Cochrane/Puerreydón and Lago General Carrera/Buenos Aires. Taking into account the volumes of water stored in these moraine dammed lake systems (Table 1) we calculate the Bayo drainage released 312 km^3 of freshwater to the Pacific Ocean.

Stage 8 11.7-8.0 ka (Fig. 15h): The final phase of lake evolution featured multiple GLOF events caused by failure of the three moraine-dammed lakes. The relative timing of the Lago Cochrane/Puerreydón and Colonia events are unconstrained but the high energy processes needed to form the flood bar at the entrance to Valle Grande (Fig. 8a), at a location that would have been inundated by the Lago Colonia lake, demonstrates that the event from Lago General Carrera must have post-dated Lago Colonia drainage. The Colonia, Cochrane and General Carrera GLOFs released 9 km^3, 37 km^3 and 94 km^3 of freshwater to the Pacific Ocean respectively.

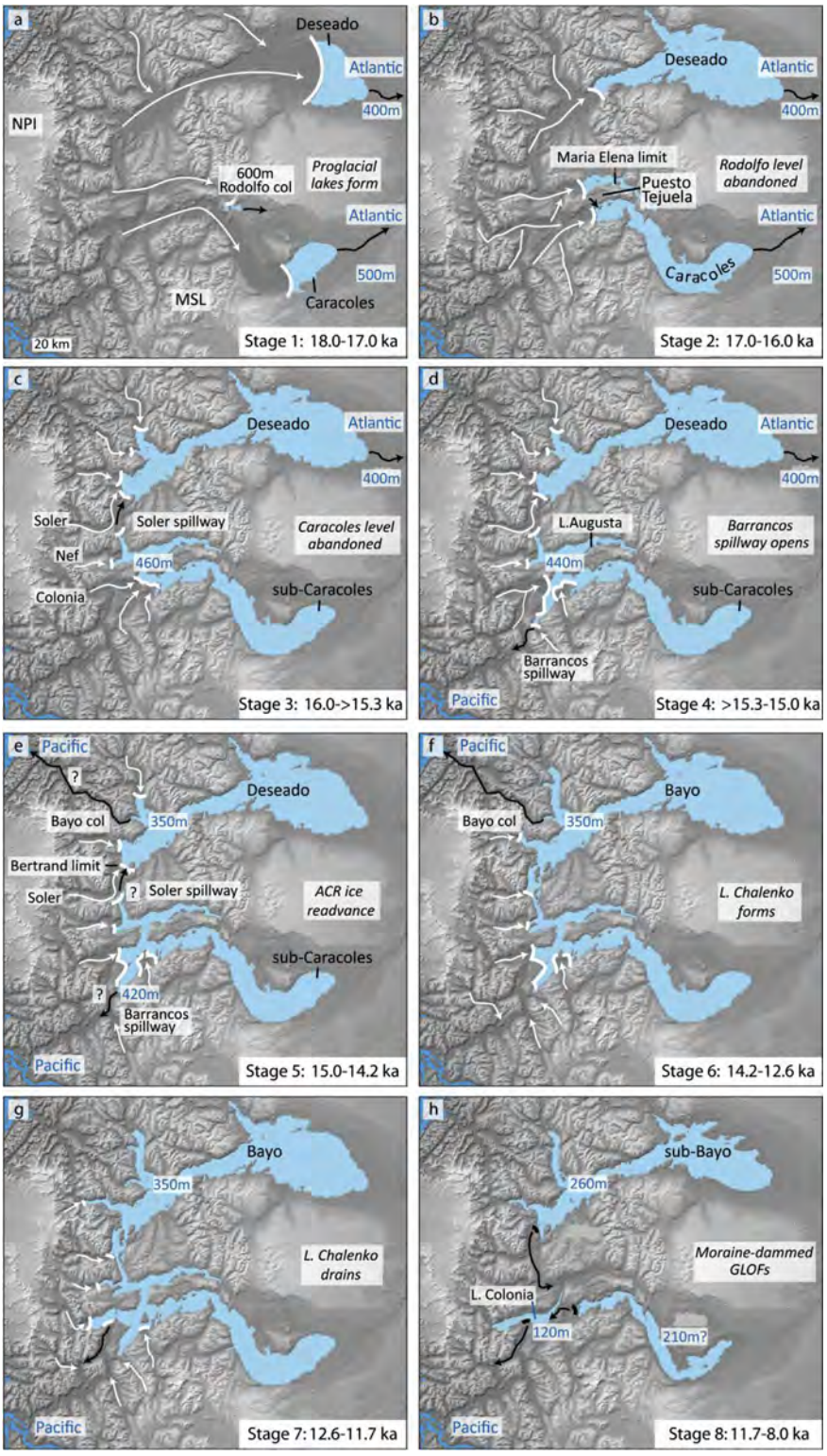

Fig. 15. Palaeolake evolution model during Patagonian Ice-Sheet deglaciation at 46–48 °S. White arrows show main ice flow pathways and black arrows meltwater drainage routes. White lines indicate glacier-lake margins, black lines mark moraine dam positions.

5.5. Late Quaternary ice sheets and continental scale drainage reversals in southernmost South America

The Baker catchment is just one of a number of river basins in Patagonia that experienced Atlantic-Pacific drainage reversals in response to the advance/retreat of glaciers during Late Quaternary glacial/interglacial cycles (Fig. 16). Caldenius (1932) reported drainage reversals from the Chabut drainage basin in northern Patagonia (41–44 °S) down to the Gallegos basin at 52°S in the South (Fig. 16). Eastward expansion of Patagonian glaciers at the

Table 3
Summary of palaeolake evolution based on modelled ages (cal ka BP). Note the lake volume and area presented in italics for stages 5 and 6 are alternative scenarios depending on lake elevation during Lago Chalenko formation. ACR = Antarctic Cold Reversal; LGC-BA = Lago General Carrera/Buenos Aires; LC-P = Lago Cochrane/Puerreydón.

Model stage	Event	Palaeolakes	Outflow elevation (m asl)	Lake level name (Fig. 10)	Drainage route (s)	Timing (cal ka BP)	Palaeolake area (km^2)	Volume drained to Pacific (km^3)
1	Ice retreat and development of proglacial lakes	L Chacabuco	620	Rodolfo	R. Pinturas (A)		Unconstrained	–
		LC-P	500	Caracoles	R. Pinturas (A)			
		LGC-BA	400	Deseado	R. Deseado (A)	18.0–17.0 ka[a]		
2	Opening of Puesto Tejuela & abandonment of Rodolfo level	L Chacabuco	520 at Puesto Tejuela	N/A	L. Chacabuco drains to LC-P and on to R.Pinturas	17.0–16.2 ka[b]	Unconstrained	–
3	Caracoles pathway abandoned	counter formatting issues	460	Sub-Caracoles	Soler ice dam to LGC-BA R. Deseado (A)	16.2–15.3 ka[c]	Unconstrained	–
4	Opening of Barrancos spillway	counter formatting issues	440–460	Sub-Caracoles	R. Baker (P)	15.3–15.0[c]	2118	37
5	Ice readvance during ACR (Bayo drainage?)		400	Deseado	R. Deseado (A)	15.0–14.2 (Phase 2)	*3366*	*109*
			350	*Bayo?*	R. Bayo (P)			
6	Formation of L. Chalenko.	L Chalenko	400	*Deseado?*	R. Deseado (A)	14.2–13.7 (Phase 3)	*5726*	*509*
			350	Bayo	R. Bayo (P)			
7	Drainage of L. Chalenko	L Chalenko	N/A	Bayo	R. Baker (P)	12.4–11.8 (Phase 4)	4424	312
8	GLOF events	LC-P	>210?		R. Cochrane -R. Baker (P)		751	37
		L Colonia	120		R. Baker (P)		153	9
		LGC-BA	260	Sub-Bayo	R. Baker (P)	9.8–8.0 (Phase 5)	2215	94

[a] Tephra constrained Fenix Chico varve record (Bendle et al., 2017b).
[b] Recaclulated Maria Elena moraine (Boex et al., 2013).
[c] Modelled Lago Augusta dates (Villa Martínez et al., 2012).

onset of glacial periods led to the damming of Pacific drainage routes. Consequently, the continental drainage divide shifted westwards to the Andean cordilleran ice divides, and meltwater drained toward the Atlantic Ocean. We estimate this westward shift in drainage encompassed an area of ~1.0×10^5 km^2 across Patagonia. The timing for the onset of this Atlantic drainage shift in the Deseado valley is poorly constrained at present but we can interpret a minimum age of 31.0–37.0 ka (MIS 3) based on OSL dates from outwash sediments to the east of Lago General Carrera/Buenos Aires (Smedley et al., 2016). García et al. (2018) dated a local LGM advance, associated with Atlantic draining outwash deposits, at ~48.0 ± 1.6 ka for the Torres del Paine and Ultima Esperanza ice lobes (51–52 °S), which provide a minimum age for Atlantic drainage down the Coyle and Gallegos river basins (Fig. 16). Pollen data from marine sediment core GeoB2107-3, located at ~27 °S to the north of the Malvinas and Brazil currents' confluence, records the presence of *Nothofagus* pollen only during the period 29-13 cal ky BP of the 73.5 ka long record (Gu et al., 2017). Efficient pollen transport by either Argentinean rivers and/or the southern westerlies into the continental margin and the Malvinas current (Fig. 1a) was hypothesised by Gu et al. (2017). Although they state a preference for wind transport we note the timing of *Nothofagus* presence fits with current constraints on a fluvial transport pathway.

Deglaciation from LGM limits led to the formation of large proglacial lakes throughout Patagonia (Fig. 16). With the exception of the rivers Santa Cruz (50°S), upper Senguer (45°S) and Negro (41°S), continued ice retreat led to Atlantic-Pacific drainage reversals with the eastward shift in the continental drainage divide towards its modern position. The reversals that led to the current configuration of the Baker and Pascua catchments, which drain to the Pacific between the northern and southern icefields, involved the capture of ~41,000 km^2 of drainage area.

The timing of palaeolake evolution in southern Patagonia can be compared to the events presented in Fig. 15. Sagredo et al. (2011) reconstructed a broadly similar temporal phasing of ice retreat and proglacial lake evolution of palaeolake Puerto Consuelo in the Ultima Esperanza fjord. Three main lake levels, at ~150, ~125 and ~30 m asl, were identified from lacustrine beach terraces and deltas in the region. The highest lake level formed in response to the start of the Last Glacial Termination (LGT, ~17.5 ka) with the first lake fall occurring by 16.1 cal ka BP (Stern et al., 2011) or 15.2 ka prior to stabilisation associated with a readvance dated to the Antarctic Cold Reversal (Sagredo et al., 2011). A subsequent lake level lowering happened between 12.8-10.3 ka. The main contrast with the Baker palaeolake model (Fig. 15) is the timing of the Atlantic to Pacific drainage reversal, which for palaeolake Puerto Consuelo occurred ~10.3 ka. To the north of Ultima Esperanza in the Torres del Paine region Solari et al. (2012) and García et al. (2014) reconstructed the history of palaeolake Tehuelche. This palaeolake was formed by the joining of Lago Sarmiento and Lago del Toro (Fig. 16) at 17.6-16.8 ka following retreat during the LGT. Drainage to the Gallegos and Atlantic Ocean was via Río Turbio (Fig. 15c), however this Atlantic drainage pathway was abandoned by the time of Antarctic Cold Reversal moraine formation with drainage inferred to the Pacific via an unknown pathway (García et al., 2014). Solari et al. (2012) report final lake drainage by ~7.1 cal yr BP. Current evidence for palaeolake histories therefore suggests a diachronous pattern across Patagonia, likely reflecting local to regional scale relief and topography.

The spatial variability in timing of drainage reversal events likely played an important role in the palaeogeography of Patagonia. The Baker and Pascua rivers, for example, now drain a large hinterland of central Patagonia (Fig. 15), and have been identified as important allochthonous sources of organic matter for ecosystems of the

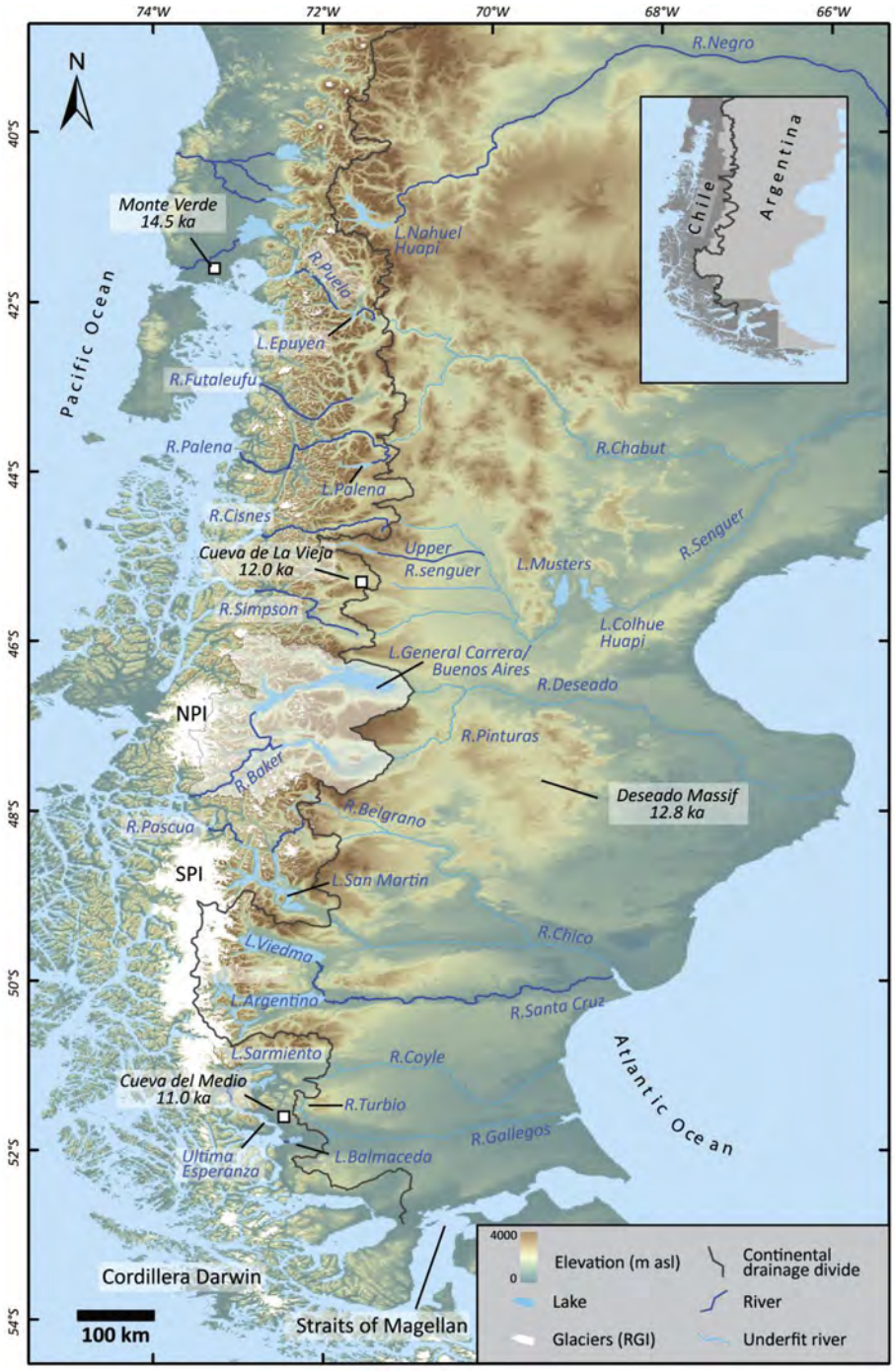

Fig. 16. Map of continental-scale drainage reversals across Patagonia and selected archaeological sites. The main drainage pathways, which experienced Atlantic-Pacific drainage reversals during PIS deglaciation, are shown by the underfit river valleys. Only ríos Negro, Santa Cruz and the upper Senguer maintained an Atlantic drainage pathway. The continental drainage divide is based on the USGS hydrosheds database (30 s South America drainage basin shapefiles). The location of the Río Baker catchment (this study) is shown. North of 46 °S, ríos Simpson, Cisnes and Futaleufu drain valleys with now disappeared palaeolakes. A major river capture event also took place at ~50 °S where Lago Viedma drained to Lago Argentino and Río Santa Cruz, abandoning its Río Chico pathway to the Atlantic. Contemporary glacier extent is from the Randolph Glacier Inventory. Inset: Map of Chile, Argentina and the continental drainage divide.

Pacific fjords (Vargas et al., 2011). By contrast it has been estimated that Patagonian rivers currently supply only 2.7% of sediment to the South Atlantic continental shelf, compared to 55.6% from coastal erosion and 41.7% from aeolian sources (Gaiero et al., 2003). In addition to possible freshwater forcing of regional climate (Glasser et al., 2016), therefore, the Atlantic-Pacific drainage reversals across Patagonia will also have affected regional sediment fluxes, and associated biogeochemical cycling, as well as water resources along river corridors in arid eastern Patagonia. The latter is potentially important for early human occupation sites across Patagonia. Brook et al. (2015) have noted, for example, that Holocene human occupation of the southern Deseado Massif was usually associated with wetter conditions. Given the timing of early human occupation in Patagonia (Fig. 15) from 14.5 ka, and possibly earlier, in the

northwest at Monte Verde (Dillehay et al., 2015), 12.8 ka in the Deseado Massif of central Patagonia (Brook et al., 2015) to ~11.0 ka at Cueva del Medio in the south (Martin and Borrera, 2017), we can hypothesise that drainage reorganisation played an important role in the palaeoenvironments encountered by early humans. Indeed lake level lowering at Ulitma Esperanza between 12.8-10.3 ka (Sagredo et al., 2011) overlaps the earliest age of human occupation of ~11.0 ka at Cueva del Medio (Fig. 15). Furthermore, the Cueva de la Vieja human occupation site (Fig. 15), dated to ~12.0 ka (Méndez et al., 2018), is located to the west of a site of Atlantic drainage abandonment, demonstrating that drainage reversals created opportunities for human occupation.

The methodological approach we have taken in this paper, therefore, provides a framework for improving understanding of Late Quaternary drainage evolution across Patagonia, with implications for the role of high magnitude floods in landscape change, freshwater forcing of regional palaeoclimate, sediment and biogeochemical fluxes, and early human occupation.

6. Conclusions

In this paper we have presented new geomorphological datasets and carried out a critical review of published geochronology from the Río Baker catchment. This has enabled the development of a Bayesian age model to underpin a reconstruction of palaeolake evolution, and Atlantic-Pacific drainage reversals, in the central Patagonian Ice Sheet (46–48ºS). Our main findings are:

1) We provide the first systematic regional data on glacio-isostatic adjustment. Histogram analysis of palaeoshoreline data shows a more comprehensive history of lake evolution than previously published models. Although the data clearly shows Lago Chalenko was unified at the Bayo level, the evidence is equivocal for the Deseado level because of previously unrecognised lake level falls in the southern basin. Our field mapping identified a new drainage pathway to the Pacific over the Barrancos col that provides geomorphological evidence for one such drainage phase.
2) We demonstrate that both the abandonment of the Caracoles outflow from Lago Cochrane/Puerreydón, and the first drainage reversal to the Pacific over the Barrancos col had occurred prior to 15.3–15.0 cal ka BP, at a time when CND ages of the Bertrand moraines (~15.9-13.7 ka) indicate a stabilised ice margin blocking the upper Baker valley. The implication is that drainage to the Pacific could originate from the southern sector of the Baker catchment independently of the northern basin.
3) The early drainage over the Barrancos col indicates that a key control on meltwater drainage pathways in the southern basin is the unzipping of ice sourced from the Northern Patagonian Icefield and Monte San Lorenzo. Previously it has been the separation of the northern and southern Patagonian icefields that was thought to control drainage through the lower Baker valley.
4) Our data do not support a Northern Hemisphere Younger Dryas/Early Holocene timing for the largest post-lLGM glacier readvance (Glasser et al., 2012). We infer a major readvance of the Soler Glacier during the Antarctic Cold Reversal. The altitudinal geochronological review and isostatic shoreline data indicate that the exposure ages of boulders dated between 10.0–12.0 ka in the Baker valley more likely date the drainage of Lago Chalenko from the Bayo level because the boulders were shielded by lake water.
5) We show that the drainage of Lago Chalenko led to the formation of a number of moraine dammed lakes following subaerial moraine exposure. These included Lago Colonia that flooded the Valle Grande basin, and lakes in the General Carrera and Cochrane basins. All three lakes drained by catastrophic GLOF events.
6) Our refined palaeolake evolution model demonstrates a total freshwater drainage of ~10^3 km^3 to the Pacific Ocean, over at least six drainage events ranging between 9 and 509 km^3. This has implications for possible freshwater forcing of regional climate as we reconstruct greater frequency of events at lower magnitudes than reported by Glasser et al. (2016).
7) The timing of Atlantic-Pacific drainage reversals from sites between 46 and 52 ºS suggests diachronous reorganisation of Patagonian drainage during Late Quaternary deglaciation of the Patagonian Ice Sheet with potential implications for early human occupation of Patagonia.

Data availability

In addition to data in Supplementary Materials, the underlying research data for the shoreline analysis (Section 3.2, Bendle, 2018) is available at https://doi.org/10.17637/rh.6480530.

Acknowledgements

VT would like to thank the Natural Resources Defence Council and Royal Holloway University of London Research Strategy Fund (RHUL-RSF) for funding initial field visits that led to this research. VT, GB and CS would like to thank Alejandro Dussaillant (Aysen University) for inviting them to the Colonia sector for two field campaigns (2011 and 2012), and Jorge Teruco for camp logistics and boating. Geovanni Daneri (Centro de Investigaciones de Ecosistemas Patagonicas) also provided logistical support for our research. JB and JM were in receipt of NERC PhD awards (NE/L501803/1 and NE/L002485/1, respectively). Cosmogenic dating (BD and VT) was supported by RHUL-RSF funding and the British Society for Geomorphology, with analysis done at the NERC-Cosmogenic Isotope Analysis Facility. ASTER GDEM is a product of NASA and METI. VT and BD were supported in the field at the Bertrand moraines by Esteban Jaramillo; GB by Xavier Ródriguez-Lloveras. We thank an anonymous reviewer and Mike Kaplan for their review comments that helped improve the original manuscript.

Appendix A. Supplementary data

Supplementary data to this article can be found online at https://doi.org/10.1016/j.quascirev.2018.10.036.

References

ASTER GDEM Validation Team, 2011. ASTER global digital elevation model version 2 – summary of validation results. In: NASA Land Processes Distributed Active Archive Center and the Joint Japan-US ASTER Science Team Report.
Baker, V.R., 2009. The channelled scabland: a retrospective. Annu. Rev. Earth Planet Sci. 37, 393–411.
Balco, G., 2011. Contributions and unrealized potential contributions of cosmogenic-nuclide exposure dating to glacier chronology, 1990 - 2010. Quat. Sci. Rev. 30, 3–27.
Balco, G., 2014. Simple computer code for estimating cosmic-ray shielding by oddly shaped objects. Quat. Geochronol. 22, 175–182.
Balco, G., Stone, J.O., Lifton, N.A., Dunai, T.J., 2008. A complete and easily accessible means of calculating surface exposure ages or erosion rates from ^{10}Be and ^{26}Al measurements. Quat. Geochronol. 3, 174–195.
Barr, I.D., Lovell, H., 2014. A review of topographic controls on moraine distribution. Geomorphology 226, 44–64.
Bell, C.M., 2008. Punctuated drainage of an ice-dammed quaternary lake in southern South America. Geogr. Ann.: Ser A Phys Geogr. 90, 1–17.
Bell, C.M., 2009. Quaternary lacustrine braid deltas on Lake General Carrera in southern Chile. Andean Geol. 36, 51–65.
Bendle, J.M., 2018. Shoreline Data. Royal Holloway University of London. https://doi.org/10.17637/rh.6480530.

Bendle, J.M., Thorndycraft, V.R., Palmer, A.P., 2017a. The glacial geomorphology of the lago Buenos Aires and lago pueyrredón ice lobes of central Patagonia. J. Maps 13, 654–673.
Bendle, J.M., Palmer, A.P., Thorndycraft, V.R., Matthews, I.P., 2017b. High-resolution chronology for deglaciation of the patagonian ice sheet at lago Buenos Aires (46.5°S) revealed through varve chronology and Bayesian age modelling. Quat. Sci. Rev. 177, 314–339.
Benn, D.I., 1996. Subglacial and subaqueous processes near a glacier grounding line: sedimentological evidence from a former ice-dammed lake, Achnasheen Scotland. Boreas 25, 23–36.
Boex, J., Fogwill, C., Harrison, S., Glasser, N., Hein, A., Schnabel, C., Xu, S., 2013. Rapid thinning of the late pleistocene patagonian ice sheet followed migration of the southern westerlies. Sci. Rep. 3, 2118.
Borrero, L.A., 2015. The process of human colonization of southern South America: migration, peopling and "the archaeology of place". J. Anthropol. Archaeol. 38, 45–51.
Bourgois, J., Cisternas, M.E., Braucher, R., Bourlès, D., Frutos, J., 2016. Geomorphic records along the General Carrera (Chile)–Buenos Aires (Argentina) glacial lake (46°–48°S), climate inferences, and glacial rebound for the past 7–9 ka. J. Geol. 124, 27—53.
Breckenridge, A., 2013. An analysis of the late glacial lake levels within the western Lake Superior basin based on digital elevation models. Quat. Res. 80, 383–395.
Breckenridge, A., 2015. The Tintah-Campbell gap and implications for glacial Lake Agassiz drainage during the Younger Dryas cold interval. Quat. Sci. Rev. 117, 124–134.
Bronk Ramsey, C., 2008. Deposition models for chronological records. Quat. Sci. Rev. 27, 42–60.
Bronk Ramsey, C., 2009. Bayesian analysis of radiocarbon dates. Radiocarbon 51, 337–360.
Brook, G.A., Franco, N.V., Ambrústolo, P., Mancini, M.V., Wang, L., Fernandez, P.M., 2015. Evidence of the earliest humans in the southern Deseado massif (Patagonia, Argentina), mylodontidae, and changes in water availability. Quat. Int. 363, 107–125.
Caldenius, C.C., 1932. Las glaciaciones cuaternarios en la Patagonia y Tierra del Fuego. Geogr. Ann. 14, 1–164.
Carling, P.A., 2013. Freshwater megaflood sedimentation: what can we learn about generic processes? Earth Sci. Rev. 125, 87–113.
Carrivick, J.L., Tweed, F.S., 2013. Proglacial lakes: character, behaviour and geological importance. Quat. Sci. Rev. 78, 34–52.
Cockburn, H.A.P., Summerfield, M.A., 2004. Geomorphological applications of cosmogenic isotope analysis. Prog. Phys. Geogr. 28, 1–42.
Condron, A., Winsor, P., 2012. Meltwater routing and the younger Dryas. Proc. Natl. Acad. Sci. Unit. States Am. 909, 19928–19933.
Darvill, C.M., 2013. Cosmogenic nuclide analysis. In: Clarke, L., Nield, J. (Eds.), Geomorphological Techniques. British Society for Geomorphology, London.
Dietrich, P., Ghienne, J.-F., Normandeau, A., Lajeunese, P., 2017. Reconstructing ic-margin retreat using delta morphostratigraphy. Sci. Rep. 7, 16936.
Dillehay, T.D., Ocampo, C., Saavedra, J., Sawakuchi, A.O., Vega, R.M., Pino, M., Collins, M.B., Cummings, L.S., Arregui, I., Villagran, X.S., Hartman, G.A., Mella, M., González, A., Dix, G., 2015. New archaeological evidence for an early human presence at Monte Verde, Chile. PloS One 10 e0145471.
Douglass, D.C., Singer, B.S., Kaplan, M.R., Mickelson, D.M., Caffee, M.W., 2006. Cosmogenic nuclide surface exposure dating of boulders on last-glacial and late-glacial moraines, Lago Buenos Aires, Argentina: interpretive strategies and paleoclimate implications. Quat. Geochronol. 1, 43–58.
Dussaillant, A.J., Buytaert, W., Meier, C., Espinoza, F., 2012. Hydrological regime of remote catchments with extreme gradients under accelerated change: the Baker basin in Patagonia. Hydrol. Sci. J. 57, 530–1542.
Durcan, J.A., King, G.E., Duller, G.A.T., 2015. DRAC: dose rate and age calculator for trapped charge dating. Quat. Geochronol. 28, 54–61.
Evans, D.J.A., Hiemstra, J.F., Cofaigh, C.Ó., 2012. Stratigraphic architecture and sedimentology of a Late Pleistocene subaqueous moraine complex, southwest Ireland. J. Quat. Sci. 27, 51–63.
Fabel, D., Small, D., Miguens-Rodriguez, M., Freeman, S.P.H.T., 2010. Cosmogenic nuclide exposure ages from the 'parallel roads' of glen roy, scotland. J. Quat. Sci. 25, 597–603.
Gaiero, D.M., Probst, J.-L., Depetris, P.J., Bidart, S.M., Leleyter, L., 2003. Iron and other transition metals in Patagonian riverborne and windborne materials: geochemical control and transport to the southern South Atlantic Ocean. Geochem. Cosmochim. Acta 67, 3603–3623.
Galbraith, R.F., Roberts, R.G., Laslett, G.M., Yoshida, H., Olley, J.M., 1999. Optical dating of single and multiple grains of quartz from jinmium rock shelter, northern Australia: Part I, experimental design and statistical models. Archaeometry 41, 339–364.
García, J.L., Kaplan, M.R., Hall, B.L., Schaefer, J.M., Vega, R.M., Schwartz, R., Finkel, R., 2012. Glacier expansion in southern Patagonia throughout the antarctic cold reversal. Geology 40, 859–862.
García, J.L., Hall, B.L., Kaplan, M.R., Vega, R.M., Strelin, J.A., 2014. Glacial geomorphology of the Torres del Paine region (southern Patagonia): implications for glaciation, deglaciation and paleolake history. Geomorphology 204, 599–616.
García, J.L., Hein, A.S., Binnie, S.A., Gómez, G.A., González, M.A., Dunai, T.J., 2018. The MIS 3 maximum of the Torres del Paine and Última Esperanza ice lobes in Patagonia and the pacing of southern mountain glaciation. Quat. Sci. Rev. 185, 9–26.
Glasser, N.F., Jansson, K.N., 2005. Fast-flowing outlet glaciers of the last glacial maximum Patagonian Icefield. Quat. Res. 63, 206–211.
Glasser, N.F., Jansson, K., 2008. The glacial map of southern South America. J. Maps 4, 175–196.
Glasser, N.F., Jansson, K.N., Harrison, S., Kleman, J., 2008. The glacial geomorphology and Pleistocene history of South America between 38°S and 56°S. Quat. Sci. Rev. 27, 365–390.
Glasser, N.F., Harrison, S., Ivy-Ochs, S., Duller, G.A., Kubik, P.W., 2006. Evidence from the Rio Bayo Valley on the extent of the north patagonian icefield during the late pleistocene-holocene transition. Quat. Res. 65, 70–77.
Glasser, N.F., Harrison, S., Schnabel, C., Fabel, D., Jansson, K.N., 2012. Younger Dryas and early Holocene age glacier advances in Patagonia. Quat. Sci. Rev. 58, 7–17.
Glasser, N.F., Jansson, K.N., Duller, G.A., Singarayer, J., Holloway, M., Harrison, S., 2016. Glacial lake drainage in Patagonia (13-8 kyr) and response of the adjacent Pacific Ocean. Sci. Rep. 6, 21064.
Gosse, J.C., Phillips, F.M., 2001. Terrestrial in situ cosmogenic nuclides: theory and application. Quat. Sci. Rev. 20, 1475–1560.
Gu, F., Zonneveld, K.A.F., Chiessi, M., Arz, H.W., Pätzold, J., Behling, H., 2017. Long-term vegetation, climate and ocean dynamics inferred from a 73,500 years old marine sediment core (GeoB2107-3) off southern Brazil. Quat. Sci. Rev. 172, 55–71.
Hall, B.L., Porter, C.T., Denton, G.H., Lowell, T.V., Bromley, G.R.M., 2013. Extensive recession of Cordillera Darwin glaciers in southernmost South America during heinrich stadial 1. Quat. Sci. Rev. 62, 49–55.
Hein, A.S., Hulton, N.R.J., Dunai, T.J., Sugden, D.E., Kaplan, M.R., Xu, S., 2010. The chronology of the last glacial maximum and deglacial events in central argentine Patagonia. Quat. Sci. Rev. 29, 1212–1227.
Henríquez, W.I., Villa-Martínez, R., Vilanova, I., De Pol-Holz, R., Moreno, P.I., 2017. The last glacial termination on the eastern flank of the central Patagonian Andes (47°S). Clim. Past 13, 879–895.
Heyman, J., Applegate, P.J., Blomdin, R., Gribenski, N., Harbor, J.M., Stroeven, A.P., 2016. Boulder height – exposure age relationships from a global glacial 10Be compilation. Quat. Geochronol. 34, 1–11.
Hogg, A.G., Hua, Q., Blackwell, P.G., Niu, M., Buck, C.E., Guilderson, T.P., Heaton, T.J., Palmer, J.G., Reimer, P.J., Reimer, R.W., Turney, C.S., 2013. SHCal13 Southern Hemisphere calibration, 0–50,000 years cal BP. Radiocarbon 55, 1–15.
Hubbard, A., Hein, A.S., Kaplan, M.R., Hulton, N.R., Glasser, N., 2005. A modelling reconstruction of the last glacial maximum ice sheet and its deglaciation in the vicinity of the Northern Patagonian Icefield, South America. Geogr. Ann.: Ser A Phys Geogr. 87, 375–391.
Hudson, P.F., Middelkoop, H., Stouthamer, E., 2008. Flood management along the Lower Mississippi and Rhine Rivers (The Netherlands) and the continuum of geomorphic adjustment. Geomorphology 101, 209–236.
Kaplan, M.R., Strelin, J.A., Schaefer, J.M., Denton, G.H., Finkel, R.C., Schwartz, R., Putnam, A.E., Vandergoes, M.J., Goehring, B.M., Travis, S.G., 2011. In-situ cosmogenic ^{10}Be production rate at Lago Argentino, Patagonia: implications for late-glacial climate chronology. Earth Planet Sci. Lett. 309, 21–32.
Lal, D., 1991. Cosmic ray labeling of erosion surfaces: in situ nuclide production rates and erosion models. Earth Planet Sci. Lett. 104, 424–439.
Martin, F.B., Borrera, L.A., 2017. Climate change, availability of territory, and late pleistocene human exploration of Ultima Esperanza, south Chile. Quat. Int. 428, 86–95.
Martinod, J., Pouyaud, B., Carretier, S., Guillaume, B., Hérail, G., 2016. Geomorphic records along the general Carrera (Chile)–Buenos Aires (Argentina) glacial Lake (46°–48°S), climate inferences, and glacial rebound for the past 7–9 ka: a discussion. J. Geol. 124, 631–635.
Mendelova, M., Hein, A.S., McCulloch, R., Davies, B., 2017. The last glacial maximum and deglaciation in central Patagonia, 44°S–49°S. In: Cuadernos de Investigacíon Geográfica.
Méndez, C., Delaunay, A.N., Reyes, O., Ozlán, I.L., Belmar, C., López, P., 2018. The initial peopling of Central Western Patagonia (southernmost South America): late Pleistocene through Holocene site context and archaeological assesmblages from Cueva de la Vieja site. Quat. Int. 473, 261–277.
Mercer, J.H., 1976. Glacial history of southernmost South America. Quat. Res. 6, 125–166.
Moreno, P.I., Kaplan, M.R., Francois, J.P., Villa-Martínez, R., Moy, C.M., Stern, C.R., Kubik, P.W., 2009. Renewed glacial activity during the Antarctic Cold Reversal and persistence of cold conditions until 11.5 ka in southwestern Patagonia. Geology 37, 375–378.
Moreno, P.I., Denton, G.H., Moreno, H., Lowell, T.V., Putnam, E., Kaplan, M.R., 2015. Radiocarbon chronology of the last glacial maximum and its termination in northwestern Patagonia. Quat. Sci. Rev. 122, 233–249.
Nimick, D.A., McGrath, D., Mahan, S.A., Friesen, B.A., Leidich, J., 2016. Latest pleistocene and Holocene glacial events in the Colonia valley, northern Patagonia icefield, southern Chile. J. Quat. Sci. 31, 551–564.
Nishiizumi, K., Imamura, M., Caffee, M.W., Southon, J.R., Finkel, R.C., McAninch, J., 2007. Absolute calibration of 10Be AMS standards. Nucl. Instrum. Methods Phys. Res. Sect. B Beam Interact. Mater. Atoms 258, 403–413.
Palmer, A., Lowe, J.J., 2017. Dynamic landscape changes in glen roy and vicinity, west highland scotland, during the younger Dryas and earyl Holocene: a synthesis. PGA (Proc. Geol. Assoc.) 128, 2–25.
Pedro, J.B., Martin, T., Steig, E.J., Jochum, M., Park, W., Rasmussen, S.O., 2016. Southern Ocean deep convection as a driver of Antarctic warming events. Geophys. Res. Lett. 43, 2192–2199.
Putkonen, J., Swanson, T., 2003. Accuracy of cosmogenic ages for moraines. Quat.

Res. 59, 255–261.
Putnam, A.E., Denton, G.H., Schaefer, J.M., Barrell, D.J., Andersen, B.G., Finkel, R.C., Schwartz, R., Doughty, A.M., Kaplan, M.R., Schlüchter, C., 2010. Glacier advance in southern middle-latitudes during the antarctic cold reversal. Nat. Geosci. 3, 700–704.
Rebassa, J., Coronato, A., Martinez, O.A., 2011. Late Cenozoic glaciations in Patagonia and Tierra del Fuego: an updated review. Biol. J. Linn. Soc. 103, 316–335.
Sagredo, E.A., Moreno, P.I., Villa-Martínez, R., Kaplan, M.R., Kubik, P.W., Stern, C.R., 2011. Fluctuations of the Última Esperanza ice lobe (52°S), Chilean Patagonia, during the last glacial maximum and termination 1. Geomorphology 125, 92–108.
Sagredo, E.A., Kaplan, M.R., Araya, P.S., Lowell, T.V., Aravena, J.C., Moreno, P.I., Kelly, M.A., Schaefer, J.M., 2018. Trans-pacific glacial response to the Antarctic Cold Reversal in the southern mid-latitudes. Quat. Sci. Rev. 189, 57–75.
Schaller, M., von Blanckenburg, F., Veldkamp, A., Tebbens, L.A., Hovius, N., Kubik, P.W., 2002. A 30 000 yr record of erosion rates from cosmogenic 10Be in Middle European river terraces. Earth Planet Sci. Lett. 204, 307–320.
Smedley, R.K., Glasser, N.F., Duller, G.A.T., 2016. Luminescence dating of glacial advances at lago Buenos Aires (~46°S), Patagonia. Quat. Sci. Rev. 134, 59–73.
Solari, M.A., Le Roux, J.P., Hervé, F., Airo, A., Calderón, M., 2012. Evolution of the Great Tehuleche Palaeolake in the Torres del Paine National Park of Chilean Patagonia during the Last Glacial Maximum and Holocene. Andean Geol. 39, 1–21.
Stern, C.R., Moreno, P.I., Villa-Martínez, R., Sagredo, E.A., Prieto, A., Labarca, R., 2011. Evolution of ice-dammed proglacial lakes in Última Esperanza, Chile: implications from the late-glacial RI eruption of Reclús volcano, Andean Austral Volcanic Zone. Andean Geol. 38, 82–97.
Stone, J.O., 2000. Air pressure and cosmogenic isotope production. J. Geophys. Res.: Solid Earth 105, 23753–23759.
Turner, K.J., Fogwill, C.J., McCulloch, R.D., Sugden, D.E., 2005. Deglaciation of the eastern flank of the north patagonian icefield and associated continental-scale lake diversions. Geogr. Ann.: Ser A Phys Geogr. 87, 363–374.
Vargas, C.A., Martinez, R.A., San Martin, V., Aguayo, M., Silva, N., Torres, R., 2011. Allochthonous subsidies of organic matter across a lake-river-fjord landcape in the Chilean Patagonia: implications for marine zooplankton in inner fjord áreas. Continent. Shelf Res. 31, 187–201.
Villa-Martínez, R., Moreno, P.I., Valenzuela, M.A., 2012. Deglacial and postglacial vegetation changes on the eastern slopes of the central Patagonian Andes (47°S). Quat. Sci. Rev. 32, 86–99.
WAIS Divide Project Members, 2013. Onset of deglacial warming in West Antarctica driven by local orbital forcing. Nature 500, 440–443.
Weller, D., Miranda, C.G., Moreno, P.I., Villa-Martínez, R., Stern, C.R., 2014. The large late-glacial Ho eruption of the Hudson volcano, southern Chile. Bull. Volcanol. 76, 831.